

Helsinki University of Technology Radio Laboratory Publications
Teknillisen korkeakoulun Radiolaboratorion julkaisuja
Espoo, September 2006

REPORT S 284

ANALYTICAL MODELLING OF METAMATERIALS AND A NEW PRINCIPLE OF SUB-WAVELENGTH IMAGING

Pavel Belov

Dissertation for the degree of Doctor of Science in Technology to be presented with due permission for public examination and debate in Auditorium S4 at Helsinki University of Technology (Espoo, Finland) on the 22nd of November 2006 at 12 o'clock noon.

**Helsinki University of Technology
Department of Electrical and Communications Engineering
Radio Laboratory**

**Teknillinen korkeakoulu
Sähkö- ja tietoliikennetekniikan osasto
Radiolaboratorio**

Distribution:

Helsinki University of Technology

Radio Laboratory

P.O. Box 3000

FI-02015 TKK

Tel. +358-9-451 2252

Fax. +358-9-451 2152

© Pavel Belov and Helsinki University of Technology Radio Laboratory

ISBN 951-22-8377-8 (printed)

ISBN 951-22-8378-6 (pdf)

URL: <http://lib.tkk.fi/Diss/2006/isbn9512283786/>

ISSN 1456-3835

Otamedia Oy

Espoo 2006



HELSINKI UNIVERSITY OF TECHNOLOGY P.O. BOX 1000, FI-02015 TKK http://www.tkk.fi	ABSTRACT OF DOCTORAL DISSERTATION
Author	
Name of the dissertation	
Date of manuscript	Date of the dissertation
Monograph	Article dissertation (summary + original articles)
Department	
Laboratory	
Field of research	
Opponent(s)	
Supervisor (Instructor)	
Abstract	
Keywords	
ISBN (printed)	ISSN (printed)
ISBN (pdf)	ISSN (pdf)
ISBN (others)	Number of pages
Publisher	
Print distribution	
The dissertation can be read at http://lib.tkk.fi/Diss/	

Nothing is as easy as it looks.
Everything takes longer than you think.
Complex problems have simple, easy to understand wrong answers.
(Murphy's Laws)

Preface

This thesis is devoted to unlimited patience of my supervisor Prof. Sergei Tretyakov. Also, I am very grateful to Prof. Constantin Simovski for cooperation, help, and discussions of the results presented in this work. A lot of thanks to my wife, Arina Beda, for understanding and support during preparation of this thesis.

Pavel Belov
22nd February 2006, London

List of publications

- [P1] P.A. Belov, Y. Hao “Subwavelength imaging at optical frequencies using a transmission device formed by a periodic layered metal-dielectric structure operating in the canalization regime”, *Physical Review B*, vol. 73, pp. 113110 (1-4), 2006.
- [P2] P.A. Belov, Y. Hao, S. Sudhakaran, “Subwavelength microwave imaging using an array of parallel conducting wires as a lens”, *Physical Review B*, vol. 73, 033108 (1-4), 2006.
- [P3] P. Ikonen, P.A. Belov, C.R. Simovski, S.I. Maslovski, “Experimental demonstration of subwavelength field channeling at microwave frequencies using a capacitively loaded wire medium”, *Physical Review B*, vol. 73, pp. 073102 (1-4), 2006.
- [P4] P.A. Belov, C.R. Simovski, “Boundary conditions for interfaces of electromagnetic crystals and the generalized Ewald-Oseen extinction principle”, *Physical Review B*, vol. 73, pp. 045102 (1-14), 2006.
- [P5] P.A. Belov, C.R. Simovski, “Subwavelength metallic waveguides loaded by uniaxial resonant scatterers”, *Physical Review E*, vol. 72, pp. 036618 (1-11), 2005.
- [P6] P.A. Belov, C.R. Simovski, “Homogenization of electromagnetic crystals formed by uniaxial resonant scatterers”, *Physical Review E*, vol. 72, pp. 026615 (1-15), 2005.
- [P7] P.A. Belov, M.G. Silveirinha, “Resolution of sub-wavelength lenses formed by a wire medium”, *Physical Review E*, vol. 73, pp. 056607 (1-9), 2006.
- [P8] P.A. Belov, C.R. Simovski, P. Ikonen, “Canalization of subwavelength images by electromagnetic crystals”, *Physical Review B*, vol. 71, 193105 (1-4), 2005 (also included into *Virtual Journal of Nanoscale Science and Technology*, vol. 11, no. 23, 2005).
- [P9] C.R. Simovski, P.A. Belov, “Low-frequency spatial dispersion in wire media”, *Physical Review E*, vol. 70, pp. 046616 (1-8), 2004.
- [P10] P.A. Belov, K.R. Simovski, S.A. Tretyakov, “Backward waves and negative refraction in photonic (electromagnetic) crystals”, *Journal of Communications Technology and Electronics*, Vol. 49, No. 11, pp. 1199-1207, 2004.
- [P11] C.R. Simovski, P.A. Belov, S. He, “Backward wave region and negative material parameters of a structure formed by lattices of wires and split-ring resonators”, *IEEE Trans. on Antennas and Propagation*, vol. 51, no. 10, pp. 2582- 2591, 2003.
- [P12] S.A. Tretyakov, S.I. Maslovski, P.A. Belov, “An analytical model of metamaterials based on loaded wire dipoles”, *IEEE Trans. on Antennas and Propagation*, vol. 51, no. 10, pp. 2652- 2658, 2003.

- [P13] P.A. Belov, S.I. Maslovski, K.R. Simovski, S.A. Tretyakov, “A condition imposed on the electromagnetic polarizability of a bianisotropic lossless scatterer”, *Technical Physics Letters*, vol. 29, no. 9, pp. 718-720, 2003.
- [P14] P.A. Belov, C.R. Simovski, S.A. Tretyakov, “An example of bi-anisotropic electromagnetic crystals: the spiral medium”, *Physical Review E*, vol. 67, 056622 (1-6), 2003.
- [P15] P.A. Belov, R. Marques, S.I. Maslovski, I.S. Nefedov, M. Silverinha, C.R. Simovski, S.A. Tretyakov, “Strong spatial dispersion in wire media in the very large wavelength limit”, *Physical Review B*, vol. 67, pp. 113103 (1-4), 2003.
- [P16] P.A. Belov, “Backward waves and negative refraction in uniaxial dielectrics with negative dielectric permittivity along the anisotropy axis”, *Microwave and Optical Technology Letters*, vol. 37, no. 4, pp. 259-263, 2003.
- [P17] P.A. Belov, C.R. Simovski, S.A. Tretyakov, “Two-dimensional electromagnetic crystals formed by reactively loaded wires”, *Physical Review E*, vol. 66, pp. 036610 (1-7), 2002.
- [P18] P.A. Belov, S.A. Tretyakov, A.J. Viitanen, “Nonreciprocal microwave bandgap structures”, *Physical Review E*, vol. 66, pp. 016608 (1-8), 2002.
- [P19] P.A. Belov, S.A. Tretyakov, “Resonant reflection from dipole arrays located very near to conducting planes”, *Journal of Electromagnetic Waves and Applications*, vol. 16, no.1, pp. 129-143, 2002.
- [P20] P.A. Belov, S.A. Tretyakov, A.J. Viitanen, “Dispersion and reflection properties of artificial media formed by regular lattices of ideally conducting wires”, *Journal of Electromagnetic Waves and Applications*, vol. 16, no. 8, pp. 1153-1170, 2002.

Contribution of the author

Papers [P1, P2, P4-P10, P13, P14, P16-P20] were mainly prepared by the author. The analytical modelling was carried out under supervision of Prof. S. Tretyakov and Prof. C. Simovski. In paper [P3] the author was responsible for the theoretical part. The author of the thesis contributed into paper [P11] as the author of the main idea of analytical modelling of a lattice of wires and split-ring resonators. The model of capacitively loaded wire dipoles in [P12] has been developed by the author. The paper [P15] appeared as a result of numerous discussions between co-authors. The author of the thesis was responsible for deduction of the quasistatic limit of the analytical model presented in [P15].

Contents

Preface	i
List of publications	ii
Table of contents	iv
Introduction	1
1 Metamaterials: a historical overview	2
1.1 Artificial dielectrics	2
1.2 Wire media	3
1.3 Artificial magnetics	4
1.4 Bi-anisotropic composites	4
1.5 Double-negative and indefinite media	5
1.6 Photonic and electromagnetic crystals	7
1.7 High-impedance surfaces	9
2 Analytical modelling of metamaterials	10
2.1 Local field approach	10
2.2 Planar arrays of resonant dipoles over conducting planes	11
2.3 Simple wire medium	11
2.4 Loaded wire medium and spiral medium	15
2.5 Two- and three-dimensional wire media	16
2.6 Three-dimensional electromagnetic crystals	18
2.7 Sub-wavelength waveguides	20
2.8 Double-negative materials	21
2.9 Backward waves and negative refraction	22
3 Sub-wavelength imaging using canalization regime	23
3.1 Preamble	23
3.2 Canalization regime in a slab of capacitively loaded wire medium	25
3.3 Lens formed by a wire medium for microwave frequencies	28
3.4 Metal-dielectric layered structure for optical frequencies	31
References	35

Introduction

Rapidly growing demand of electromagnetic materials with various exotic properties is preconditioned by continuous development of novel technologies. Electromagnetic properties of naturally available media are restricted by physical reasons, that is why strong progress in studies of artificial materials (also called as metamaterials) is observed during last years. These complex materials allow us to achieve extraordinary electromagnetic properties which are sometimes even not available in natural materials. Such properties offer brilliant applications in microwave and radio engineering, optics and spectroscopy, covering the frequency region from microwaves to visible range. The regularly generated novel ideas expand this rapidly developing scientific area with extremely high rate, and promising effects attract researchers from communities which stand aside from electromagnetics, like acoustics, hydrodynamics, mechanics, etc. The most promising possibility offered by metamaterials is sub-wavelength imaging, a possibility to overcome the diffraction limit (the general restriction on resolution of conventional lenses). The technique of light manipulation using photonic crystals (superprism effect, bending waveguides, cavity resonators) and ultra-thin high-impedance coverings (magnetic conductors) which already have found numerous applications are noteworthy as well. A detailed overview of mentioned above effects, properties and applications is presented in the first part of the thesis.

The emphasis of the present work is on analytical modelling of metamaterials. This makes it different from other existing studies which are mainly based on numerical simulations and experiments. The local field approach is used as the main modelling technique. A wide variety of different metamaterials has been simulated with the help of this unique method: starting from planar grids of resonant scatterers over ground plane which behaves as an impedance surface and finishing with two and three-dimensional lattices with complex inner geometry and extraordinary dispersion properties. The trait of this approach is implementation of complex mathematical manipulations related with summation of non-convergent series using the Poisson summation formula, singularity cancelation and convergence enhancement. The goal of such transformations is to get analytical expressions which allow simple and effective numerical calculations. An overview of the main results is presented in the second part of the thesis. It is supported by references to the papers (attached to this work) where detailed explanations of the results are available. The last part of the thesis is devoted to studies of an original regime of sub-wavelength imaging which is called canalization. A short overview of recent analytical, numerical and experimental results is presented.

1 Metamaterials: a historical overview

The naturally available materials have some restrictions on their electromagnetic properties. Such materials are generally lossy and their material parameters are frequency dependent. Sometimes, it is quite hard to find a natural material which has necessary values of material parameters required for certain applications. This problem usually can be solved by using artificially manufactured materials (metamaterials). These materials are specially designed to have necessary electromagnetic properties. Some authors associate term ‘metamaterials’ with double-negative media only. In the present work the general meaning of term ‘metamaterials’ is used. By this definition the metamaterials are artificially created media with exotic electromagnetic properties which are usually not available in nature.

1.1 Artificial dielectrics

The first ever known metamaterials are artificial dielectrics. These materials mimic natural materials. They usually consist of artificially created ‘molecules’: dielectric or metallic inclusions of a certain shape (see Fig. 1). These ‘molecules’ can be distributed and oriented

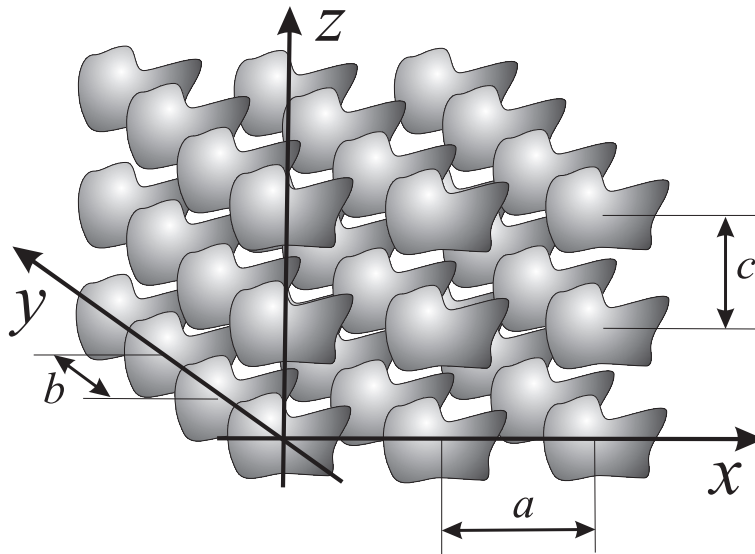


Figure 1: The geometry of a generic artificial dielectric

either regularly or chaotically. The dimensions of the ‘molecules’ and characteristic distances between neighboring ones are assumed to be small as compared to the wavelength. From the other hand, the size of a single inclusion usually is much larger than the sizes of real molecules and lattice periods of the natural material from which the artificial ‘molecule’ is composed. This allows us to describe the inclusions in terms of material parameters which fits the problem into the area of the classical electrodynamics.

The first artificial dielectric was invented by W.E. Kock [1] and used in the design of low-weight dielectric lenses at microwave frequencies. The artificial dielectrics have numerous advantages as compared to natural ones. From one hand, they can be designed to have as high permittivity as it is required for certain application and very low losses at the same time. From the other hand, the losses can be artificially enhanced and absorbing materials with high losses can be created. Also, artificial dielectrics usually have significantly reduced density which is very important in the design of both dielectric lenses and absorbers at microwave frequencies. More details about artificial dielectrics as well as extensive reference lists are available in Sec. 12 of [2], and [3].

1.2 Wire media

A very interesting example of artificial dielectrics is the wire medium [4–9] (also called “rodded medium”) known since 1960-s. It is a material formed by a regular lattice of conducting wires with small radii as compared to the lattice periods, see Fig. 2. Wire medium

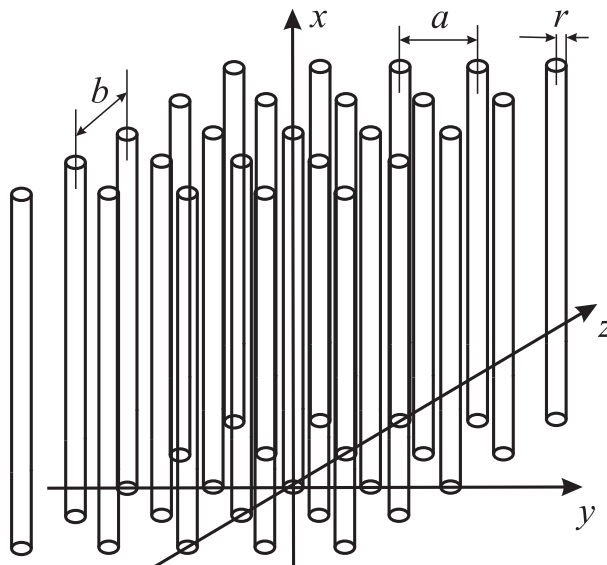


Figure 2: The geometry of wire medium: a lattice of parallel conducting thin wires.

has plasma-like frequency dependent permittivity: negative below the plasma frequency, and positive but smaller than unity above. That is why it is often called “artificial plasma” since the ideal (collisionless) electron plasma is described by permittivity of the same form. Wire media were even used for plasma simulations [10] at microwaves. Recently, the wire medium was re-discovered by J.B. Pendry [11] which initiated a new wave of the interest to this material [12, 13]. The wire medium is a unique non-resonant artificial dielectric which has negative permittivity in a very wide frequency range. This property defines the area of its applications. The wire medium was used as one of the components for creation of double-

negative media [14] (see the section about double-negative media below). Also, the wire medium was used in synthesis of high-impedance surfaces [15].

1.3 Artificial magnetics

Artificial magnetics have no shorter history than artificial dielectrics. The most popular in the present time artificial magnetics are described in details in [16], but they have been known long time before that, since 1950-s [17–19]. Artificial magnetics are usually composed from elements which have resonant magnetic response. The typical magnetic elements are split-ring resonators (see Fig. 3.a) and Swiss rolls (see Fig. 3.b). The split-ring resonators are more widely used than Swiss rolls since they can be manufactured using printed circuit board technology. An artificial magnetic formed by split-ring resonators possesses negative

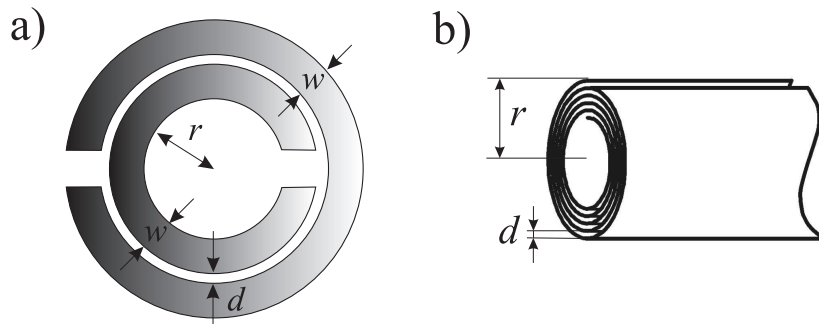


Figure 3: Components of artificial magnetics: a) split-ring resonator and b) Swiss roll [16].

permeability within a narrow frequency band near the resonant frequency of the single split-ring resonator. That is why this material is used as one of components for creation of double-negative media [14] (see the section about double-negative media below). Metallic waveguides filled by such artificial magnetics support guided waves at frequencies below the cutoff frequency of hollow waveguides which makes the waveguides sub-wavelength [20]. This effect is used for miniaturization of guiding structures [21].

1.4 Bi-anisotropic composites

Lattices of inclusions with a complex shape (chiral and omega particles, etc., see Fig. 4) cannot be described in terms of permittivity and permeability only, since they exhibit electromagnetic coupling. Electric field causes not only electric polarization of such media, but also magnetic, as well as magnetic field causes both magnetic and electric polarizations. Such materials are called bi-anisotropic media [22–25]. In paper [26] it was shown that even split-ring resonators (see Fig. 3.a) possess strong bi-anisotropic properties since the dimensions of the two split rings are different. This effect is harmful for creation of uniaxial artificial

magnetics discussed in the previous section. This problem was solved by introduction of double split-ring resonators formed by rings with identical sizes [26, 27].

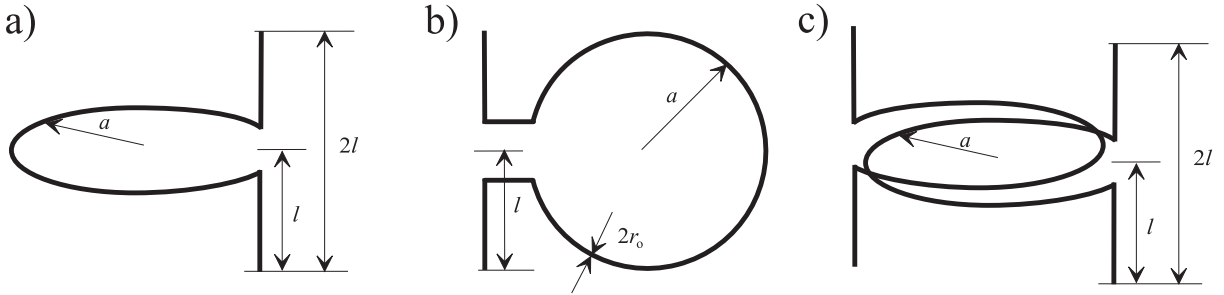


Figure 4: Bi-anisotropic particles: a) chiral, b) omega, c) double chiral [28]

The bi-anisotropic medium is the most general kind of materials which can be described in terms of local material parameters. They found application as radar absorbing materials (stealth technology) and polarization transformers. Recently, also, the negative refraction effect was reported for chiral materials [29–31].

The author of the present work has defended his MSc thesis about interaction in two-dimensional regular grids of bi-anisotropic particles. The thesis was based on works [32–39].

1.5 Double-negative and indefinite media

A special place within metamaterials is occupied by double-negative media (DNG), materials with both negative permittivity ϵ and permeability μ . Growing interest in these exotic media



Figure 5: Prof. Victor G. Veselago on the left with Prof. Ari Sihvola on the right, coining the name “Veselago medium” (Espoo, Finland, 2002)

was excited only very recently by paper [40] of J.B. Pendry [41], in spite of the fact that DNG were described by V.G. Veselago in his work [42] in 1968. In the literature, materials with negative permittivity and permeability are often called as left-handed media [14,43–45] following the original term proposed by V.G. Veselago [42], but in this thesis the term double-negative media [46,47] is used. Sometimes, DNG are also called as backward-wave media [48,49], negative-index materials [50,51], or even Veselago media, see Fig. 5. Double-negative media attract attention due to very interesting possible applications. For example, a possibility of perfect lens construction was predicted by Pendry in [40] (see the section about sub-wavelength imaging below) and a sub-wavelength cavity resonator was invented by Engheta in [52]. Plane electromagnetic waves in double-negative media are backward: the wave vector and the Poynting vector are oriented in the opposite directions (the group velocity is negative). As a result, the negative refraction effect is observed at interfaces between isotropic dielectrics and double-negative media. A possibility of negative refraction and backward-wave effects has been known since 1904 [53–58], long time before the discovery of DNG. In 1940 Russian academician L.I. Mandelshtam (see Fig. 6) even read lectures about



Figure 6: Academician L.I. Mandelshtam (1879-1944)

a possibility of negative refraction and backward waves at the physical faculty of Moscow State University [59]. The studies of double-negative materials have been continued and developed very rapidly in the present time, see special issues [60–62] and overviews [63–66]. Extensive lists of publications and additional information about double-negative materials are available at on-line resources [41,67–69].

The group of R. Shelby and D. Smith [67] offered a realization of a uniaxial version of double-negative medium [14] with the help of a lattice of wires and resonant magnetic scatterers, see Fig. 7. In their design a lattice of wires (wire medium) is responsible for negative permittivity, and a lattice of split-ring resonators allows one to create negative permeability.



Figure 7: Realization of double-negative material at microwave frequencies [43]

Negative refraction in the Shelby-Smith structure was experimentally proven [43, 51, 70] at microwave frequencies. To the present time double-negative media with such design are created for frequencies up to tetrahertz region [71, 72] and even an isotropic geometry is proposed [73]. The Shelby-Smith structure is not a unique design of double-negative media. There are also other possible realizations, like [47, 74–76].

An intermediate position between artificial dielectrics and magnetics, and double-negative media is occupied by so-called indefinite media in which the principal components of the permittivity and permeability tensors have different signs. Such materials were studied in [77–79] where a variety of effects including negative refraction, backward-wave effect, near-field focusing were demonstrated. Anisotropy of the media introduces additional freedom in manipulation of its dispersion and reflection properties [48].

1.6 Photonic and electromagnetic crystals

Artificial dielectrics operate at long wavelengths as compared to the lattice periods. In such regime the inclusions interact mainly quasi-statically. A completely different situation appears in the case of so-called electromagnetic crystals [80, 81] operating at higher frequencies where interaction between inclusions is dynamic. Electromagnetic crystals are artificial periodic structures operating at the wavelengths comparable with their period. In the optical frequency range they are called photonic crystals [82–86]. The inherent feature of such media is the existence of frequency bands where the material does not support propagating waves. These bands are called bandgaps, and therefore these crystals are sometimes called electromagnetic or photonic bandgap structures. The bandgaps are caused by spatial resonances appearing in the crystal and strongly depend on the direction of propagation. It means that electromagnetic crystals are media with spatial dispersion [87–89]. Material parameters for

such media depend on the wave vector as well as on the frequency (if they can be introduced at all). The homogenization approach is not the most convenient way for the description of electromagnetic crystals. It requires introduction of additional boundary conditions in order to describe boundary problems correctly, and this involves some related complexities.

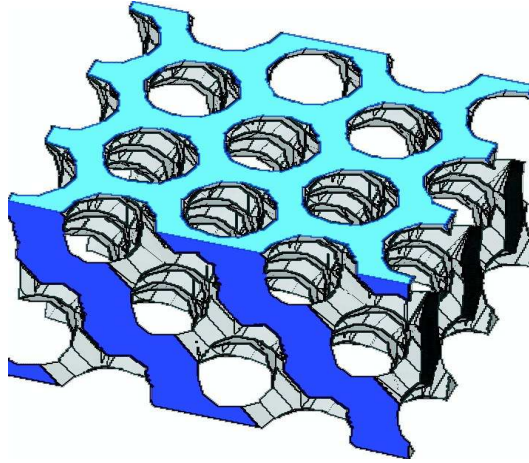


Figure 8: The first photonic crystal with a complete bandgap (yablonovite) [90]

The interest to photonic crystals arose about eighteen years ago. The start for investigations of photonic crystals was given by pioneer works [91,92] of E. Yablonovitch [93] and S. John [94] in 1987 reporting strong localization of photons and inhibited spontaneous emission due to electromagnetic bandgaps. Note, that a detailed investigation of the effect of a photonic bandgap on the spontaneous emission of embedded atoms and molecules has been performed by V. P. Bykov [95,96] fifteen years earlier. The first studies and demonstration of a photonic crystal with a complete bandgap (see Fig. 8) were done by E. Yablonovitch et al. in early 1990-s [90,97–100]. Now photonic and electromagnetic crystals have found numerous applications in frequency-selective devices, as waveguide and resonator components, in both optical and microwave ranges [80–86]. They attract attention of researchers due to very promising possibilities of light manipulation which become possible with their help [101]. Extensive lists of publications and additional information about photonic crystals are available at on-line resources [41,93,94,102,103].

Electromagnetic crystals are usually studied with the help of numerical methods [80,81,84,86] such as FDTD (finite difference time domain) and MoM (method of moments), as well as Pendry’s method [104] (which uses the condition of the field quasi-periodicity in the crystal in order to reduce the problem to numerical solution of Maxwell’s equations for one elementary cell) and Bloch-Floquet method [82,83] (based on expansion of the field into spatial harmonics). Analytical models exist only for a very narrow class of electromagnetic crystals. There are only few geometries which can be solved rigorously, and some types of electromagnetic crystals can be studied analytically only using certain approximations.

1.7 High-impedance surfaces

High-impedance surfaces (HIS) are thin composite layers at the upper surface of which impedance boundary conditions hold. If the impedance is high enough then the reflection coefficient (with respect to electric field) from the surface happens to be close to +1 and the HIS behaves as a magnetic wall. That is why HIS are also called as artificial magnetic surfaces. The most well-known sample of HIS is the simple mushroom structure [105], see Fig. 9. The structure is a composite layer that contains a periodical array of metal pins connected

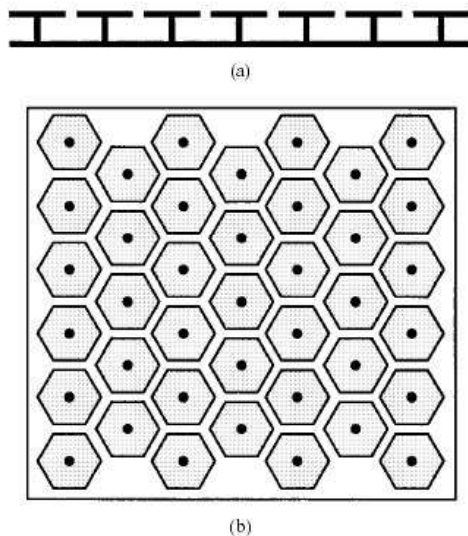


Figure 9: Geometry of simple mushroom structure [105]

to the ground and metal patches (hats). Its response to the incident electromagnetic wave can be roughly modelled as that of a resonant parallel LC-circuit. There is a modification of the mushroom structure with two-level hats [106] which allows one to significantly decrease the frequency of operation for the fixed thickness of the structure and to make it tunable. There is a number of other HIS realizations which are not suitable for wide practical applications due to complexity in manufacturing. The exceptions are screens with complex-shape slots suggested and studied in [107], but these screens are very penetrable for radiation at the resonance that restricts possible applications.

The most promising application of high-impedance surfaces is preconditioned by the fact that the interaction of horizontal antennas with HIS is constructive (in contrast to the interaction with ordinary metallic screens which is destructive). Also, besides of the magnetic wall effect for waves, the HIS can suppress (in a certain frequency band) surface waves. Thus, HIS are prospective candidates for screening of near field and reduction of specific absorption rate (SAR) keeping antenna efficiency to be high enough [108]. More detailed information about HIS is available in [109].

2 Analytical modelling of metamaterials

2.1 Local field approach

The local field approach is usually associated with the question of the local field in dielectrics, the Maxwell Garnett approximation [110] and formulae of Clausius-Mossotti and Lorenz-Lorentz, see for example [111]. It allows one to show that the effective polarizability of a molecule in a dielectric differs from its own polarizability due to interaction with other molecules, because it is affected by the local electric field which is different from the averaged one. Following deduction of Lorentz, the contribution of the interaction effect can be expressed with the help of an interaction constant which relates contribution into the local field produced by other molecules with the dipole moment of the molecule. Evaluation of the static interaction constant for different crystal lattice geometries is available in [2].

For some natural dielectrics: crystals, fluids, etc., the theory described above does not give good quantitative agreement, because the modelling of molecules by electric dipoles is inaccurate. At the same time, artificial materials can be modelled with help of local field theory with much better success. The known geometry of scatterers which form the artificial material allows one to appraise applicability of the dipole approximation. In the case if the scatterers are small as compared to the lattice periods, the local field theory gives excellent correspondence with experiment, but in the case of less compact inclusions more complicated methods should be applied [3].

In the papers included into this thesis the local field approach is used in the following formulation. Considering periodical structures formed by inclusions of a certain shape one can replace the inclusions by elementary scatterers (electrical or magnetic dipoles, lines of current) if the characteristic sizes of inclusions are smaller than wavelength. Then, the dipole moments or effective currents of the elementary scatterers can be expressed using local polarizabilities or susceptibilities through the local fields acting on the inclusions, and the field produced (scattered) by the inclusions is assumed to be equal to the field produced by these elementary scatterers. This approach allows us to separate the problem of regular structure of complex-shaped inclusions into the two separate problems: the problem of excitation of a single inclusion by local electromagnetic fields and the problem of interaction of elementary scatterers in regular arrays. These two problems are significantly easier to solve as compared to the original one.

The local field approach in this formulation has been proposed by S.A. Tretyakov in his Doctorate thesis [112] where it was successfully applied for modelling of structures formed by bi-anisotropic scatterers. Also, it is one of the basic approaches used in the book [113].

2.2 Planar arrays of resonant dipoles over conducting planes

The topic of resonant reflection from dipole arrays located very near to conducting planes was considered in paper [P19]. Plane-wave reflection from regular arrays of small particles positioned very near to an ideally conducting plane (see Fig. 10) is theoretically studied. A method to realize extremely thin resonant coverings of ideally conducting bodies which can provide resonance response and realize artificial magnetic surfaces is proposed. It has been shown that this goal can be achieved using regular arrays of small dipole antennas loaded by bulk inductive loads. Such two-dimensional regular grids of loaded wires placed over an ideally conducting plane have been studied in detail. A simple analytical theory for plane

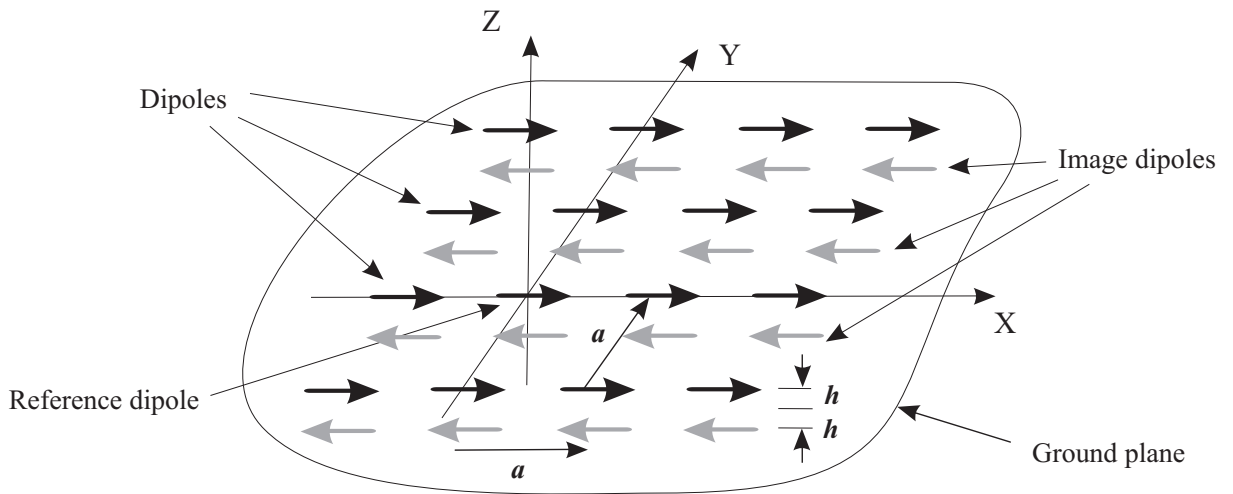


Figure 10: Planar array of dipoles over ground plane [P19].

electromagnetic wave reflection from this structure has been presented for normal incidence. From this theory it follows that the structure possesses a sharp resonance of the reflection coefficient. At resonance the reflection coefficient from the grid equals to +1. Thus, this structure behaves as a magnetic screen near the resonance, instead of an electric one as for frequencies far from the resonance. Analytical formulae for calculation of the resonant frequency and the resonance curve width are given. It turns out that this resonant frequency is smaller than the loaded wires resonant frequency, due to field interactions between the particles and the ground plane. Numerical calculations of reflection coefficient for structure with some realistic parameters have been done and dependencies of the reflection coefficient and its phase on the frequency have been plotted.

2.3 Simple wire medium

Following the local field approach the simple wire medium (Fig. 2) formed by thin wires can be treated as a grid of linear currents flowing along the axes of the wires. This approximation

is accurate while the transverse polarization of wires can be neglected (radii of wires are smaller than the lattice periods and the wavelength). The susceptibility of a single wire (the ratio between the induced current and the applied electric field) can be easily obtained using an expression for the field produced by a linear current available at [114], see [P20] for details. The interaction between the linear currents in the grid can be described using the dynamic interaction constant concept. This constant is the ratio between the local electric field created by the phased grid at the place of location of the reference wire and the current in the reference wire. The dynamic interaction constant depends on the frequency, the wave vector and the periods of the lattice. It can be evaluated using the Poisson summation formula for improvement of series formed by Green's functions describing field produced by a single wire in the same manner as it has been done for planar arrays of wires in [115–117], see [P20] for details. As a result, an analytical transcendental dispersion equation for the wire medium has been obtained in [P20]. This equation allows us to study dispersion properties of wire medium considering it as an electromagnetic crystal. Under the local field approximation only the radius of wires has to be much smaller than the wavelength and the periods of the lattice, but the wavelength can be comparable with the lattice periods and thus, the spatial resonances of the lattice can be studied without any additional efforts. Typical dispersion curves obtained in [P20] are presented in Fig. 11. The low frequency bandgap for extraordinary modes is clearly visible. Using these results, the reflection problem from an

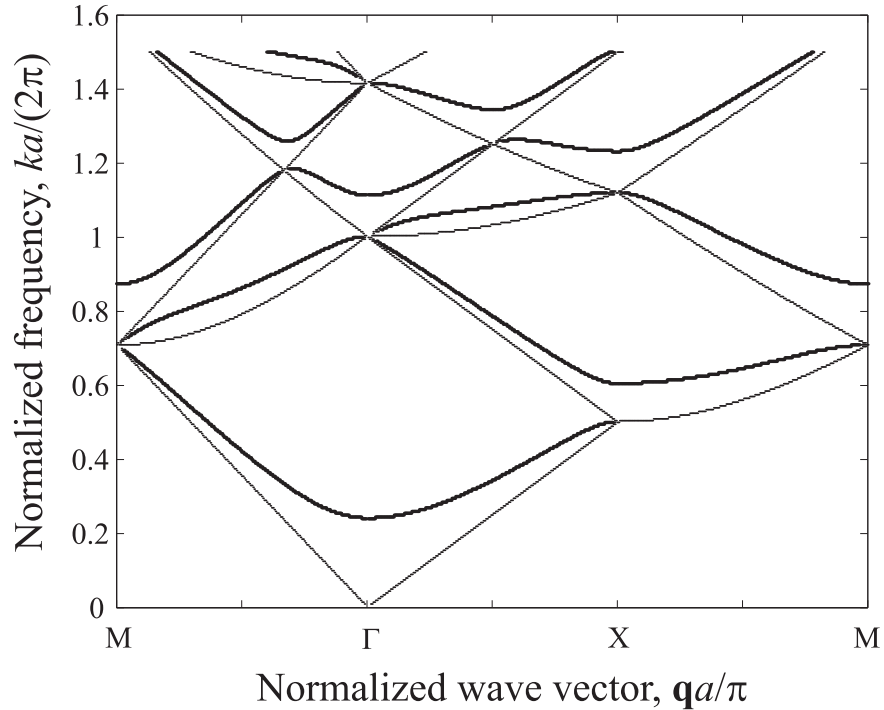


Figure 11: Dispersion curves for the wire medium with the filling ratio $f = 0.001$: thick lines - extraordinary modes, thin lines - ordinary modes. [P20]

interface between a half space of wire medium and free space is solved in [P20] for plane-wave excitation. It is shown that at the plasma frequency the interface operates as a magnetic screen (reflection coefficient for the electric field is equal to +1).

In paper [P15] it is shown that the wire medium supports three different types of modes, in contrast to the usual uniaxial dielectrics which support two types of modes: ordinary and extraordinary:

- TE modes (transverse electric with respect to the wires, or ordinary modes), the waves which polarize wires across and do not induce any currents along the wires. In thin wire approximation one can say that these are the modes which travel in free space and do not interact with the wires.
- TM modes (transverse magnetic with respect to the wires, or extraordinary modes), the waves which correspond to nonzero currents in the wires and nonzero electric field along the wires. These modes are described by a transcendental dispersion equation available in [P15, P20]
- TEM modes (transverse electric and magnetic with respect to the wires, or transmission-line modes), the waves with nonzero currents in the wires, but with zero electric field along the wires. These modes travel with the speed of light along the wires and can have any wave vector in the transverse direction. Effectively, these waves corresponds to the modes of a multi-conductor transmission line formed by the wires.

The presence of TEM (transmission-line) mode is an evidence of strong spatial dispersion in wire media. In paper [P15] it is shown that the spatial dispersion is inherent to the wire medium even at very low frequencies (see also [118] where the wire medium is considered as a limiting case of an array of aligned fibers with material parameters tending to infinity). Usually, effects of spatial dispersion can be observed in crystals at the frequencies corresponding to spatial resonances when the wavelength in free space is comparable with the periods of the structure (usual photonic and electromagnetic crystals [80–86]), or when the wavelength in the crystal becomes comparable with the periods of the structure due to resonant behavior of inclusions like in the case of resonant artificial dielectrics [119] or photonic crystals made from self-resonant inclusions [120]. The wire medium is a unique material where spatial dispersion is observed at very low frequencies and without any resonant effects.

In the quasi-static limit the wire medium can be described by relative dielectric permittivity of the form [P15]:

$$\bar{\epsilon} = \epsilon(\omega, q_x)\mathbf{xx} + \mathbf{yy} + \mathbf{zz}, \quad \epsilon(\omega, q_x) = 1 - \frac{k_0^2}{k^2 - q_x^2}, \quad (1)$$

where x -axis is oriented along the wires (see Fig. 2), q_x is the x -component of the wave vector $\mathbf{q} = (q_x, q_y, q_z)^T$, $k = \omega/c$ is the wave number of the host medium, c is the speed of light, $k_0 = \omega_0/c$ is the wave number corresponding to the plasma frequency ω_0 . The spatial dispersion effect is taken into account by dependence of permittivity on the wave vector component q_x along the wires which makes permittivity a non-local parameter. The conventional local dielectric permittivity [4–11] has the form:

$$\varepsilon = 1 - \frac{\omega_0^2}{\omega^2}.$$

Inconsistency of the local model for parallel wire media with non-vanishing wave-vector component along the wires has been shown in [P15]. Dramatic differences in the predicted behavior of the media described by the conventional local and the non-local model for the permittivity are shown. Finally, the proposed non-local model for the permittivity has been found to be suitable also for the description of the transmission-line modes of the structure.

Eq. (1) is the material equation in the spectral domain. The material equation in the space-time domain can be formulated either in the differential form:

$$\left[\frac{1}{c^2} \frac{\partial^2}{\partial t^2} - \frac{\partial^2}{\partial x^2} \right] (D_x(\mathbf{r}, t) - \varepsilon_0 E_x(\mathbf{r}, t)) + \varepsilon_0 k_0^2 E_x(\mathbf{r}, t) = 0. \quad (2)$$

or in the integral form:

$$D_x(x, y, z, t) = \varepsilon_0 E_x(x, y, z, t) + \frac{\varepsilon_0 k_0^2 c}{2} \int_{-\infty}^t \int_{x-c(t-t')}^{x+c(t-t')} E_x(x', y, z, t') dx' dt'. \quad (3)$$

The plasma wave number k_0 can be expressed using the following formula [P14]:

$$k_0^2 = \frac{2\pi/s^2}{\log \frac{s}{2\pi r} + F(u)}, \quad (4)$$

where $s = \sqrt{ab}$, $u = a/b$, a and b are periods of the wire medium (see Fig. 2), r is radius of wires, and

$$F(u) = -\frac{1}{2} \log u + \sum_{n=1}^{+\infty} \left(\frac{\coth(\pi n u) - 1}{n} \right) + \frac{\pi u}{6}. \quad (5)$$

For the commonly used case of the square grid ($a = b$), $F(1) = 0.5275$. Expression (4) looks similar to the approximate expressions for the plasma frequency developed earlier in [4, 10, 11, 15], but for thin wires it is more accurate and takes into account the geometry of the rectangular lattice. This fact has been demonstrated in [121] where also an expression for the plasma frequency of the wire medium formed by thick wires is available.

2.4 Loaded wire medium and spiral medium

Two-dimensional electromagnetic crystals formed by rectangular lattices of thin ideally conducting cylinders periodically loaded by bulk reactive impedances, so-called capacitively loaded wire media, see Fig. 12.a, are considered in [P17]. An analytical theory of disper-

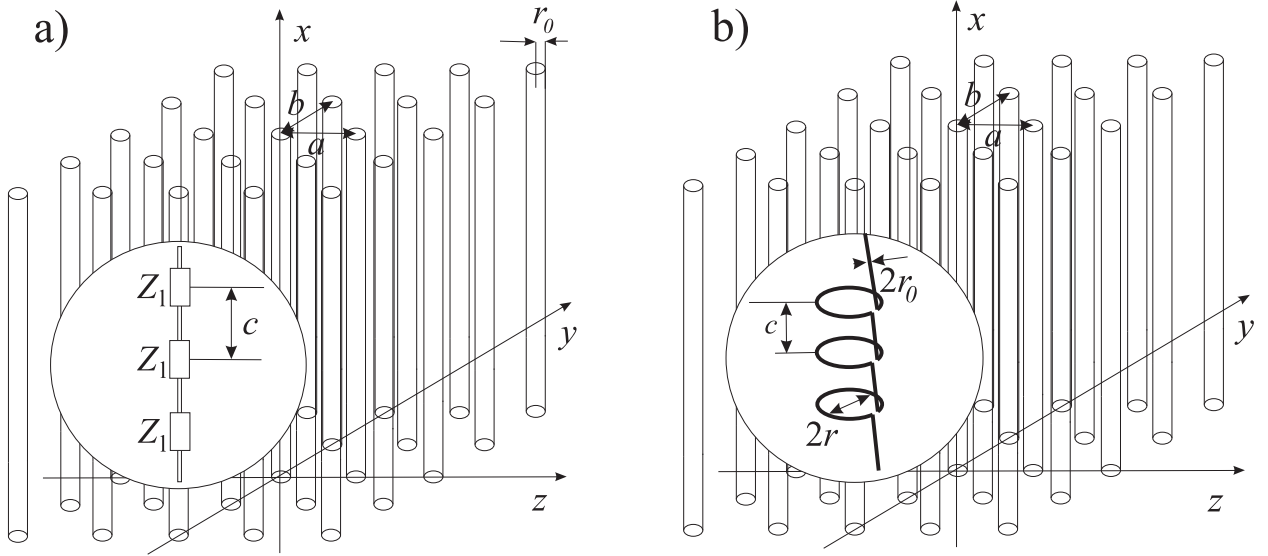


Figure 12: a) Capacitively loaded wire medium [P17] and b) spiral medium [P14].

sion and reflection from these media using the same method as in [P20] is presented. The consideration is based on the local field approach. New opportunities offered by periodical loading of wires are discussed. The transcendental dispersion equation is obtained in closed form and solved numerically. Different types of the loads like inductive, capacitive, serial and parallel LC circuits are considered. Typical dispersion curves and reflection coefficients are calculated and analyzed. It has been found that capacitive loading makes the crystal an ordinary artificial dielectric at low frequencies without any changes of the properties at high frequencies (see Fig. 13.a). Inductive loading is equivalent to an effective reduction of the wire radius and makes the low-frequency stopband narrower, but on the other hand it helps to position the upper edge of the first stopband (where the interface has very interesting for applications reflection properties) to lower frequencies. Resonant LC -circuit loading creates a resonant passband (see Fig. 13.b) and very interesting reflection properties which are rather sensitive to the position of the circuit resonance. All the described electrically controllable crystals can be successfully used in the microwave regime, for example, as elements of polarization sensitive microwave filters, antenna reflectors, and lenses. The quasi-static limit has been studied, which has resulted in a simple analytical formula for the permittivity.

The electromagnetic properties of bi-anisotropic electromagnetic crystals are studied in [P14] using an example of spiral media formed by rectangular lattices of perfectly conducting

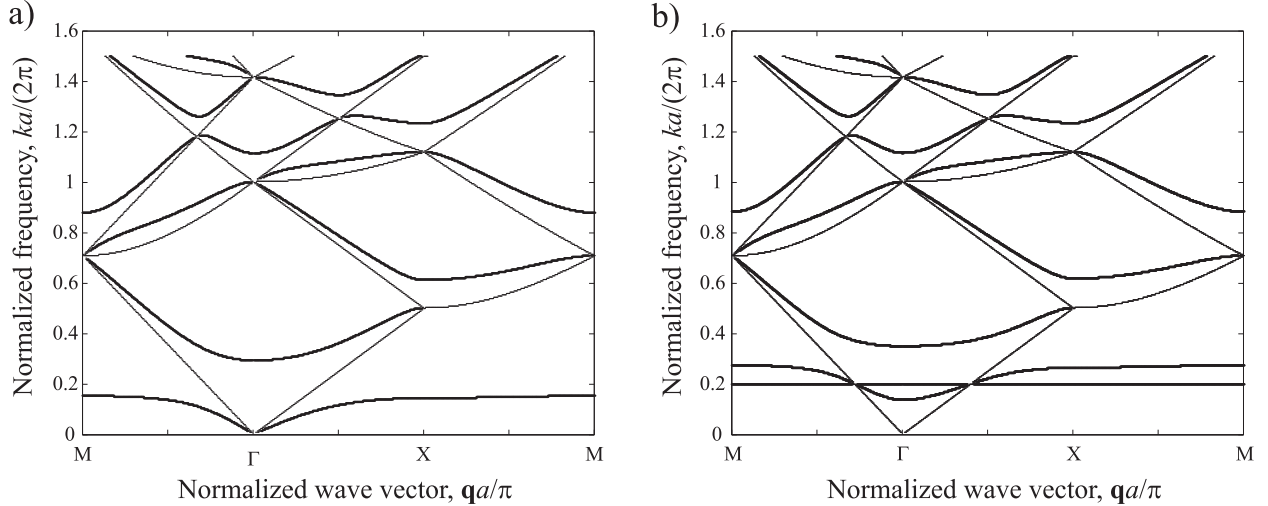


Figure 13: Dispersion diagrams for wire media loaded by: (a) capacitances, (b) parallel LC circuits [P17].

spirals, see Fig. 12.b. The analytical theory of dispersion and plane-wave reflection refers to the case when the spiral pitch and the radius are small compared to the wavelengths in the host medium. Periods of the lattice can be arbitrary. Explicit closed-form expressions are derived for the effective material parameters of the medium for the low frequency regime. The medium eigenmodes are elliptically polarized, and one of them propagates without interaction with the spirals. As to the other eigenmode, the medium has strong spatial dispersion even at extremely low frequencies in the direction along the spiral axes. Chirality factor of the medium is also very high at low frequencies. The low frequency bandgap is observed. At the frequency corresponding to its upper edge the interface of the half-space filled by the medium behaves as a magnetic wall for one of the eigenmodes. This frequency is the lower edge of the mini-band related with the spiral antiresonance. Within this mini-band there is a frequency at which the spiral medium is completely transparent in all directions. At the frequencies higher than the antiresonance, a stopband with strong spatial dispersion in the directions perpendicular to the spiral axes appears. Numerical examples are given for dispersion plots, plots of the reflection coefficient and the material parameters. A straightforward analogy between the spiral medium and the wire medium loaded by parallel LC circuits [P17] is indicated.

2.5 Two- and three-dimensional wire media

Paper [P9] is dedicated to the theoretical analysis of wire media, i.e. lattices of perfectly conducting wires comprised of two or three doubly periodic arrays of parallel wires which are orthogonal to one another [122–124], see Fig. 14 (the diamond-like structure has been considered in [125]). An analytical method based on the local field approach is used. Ex-

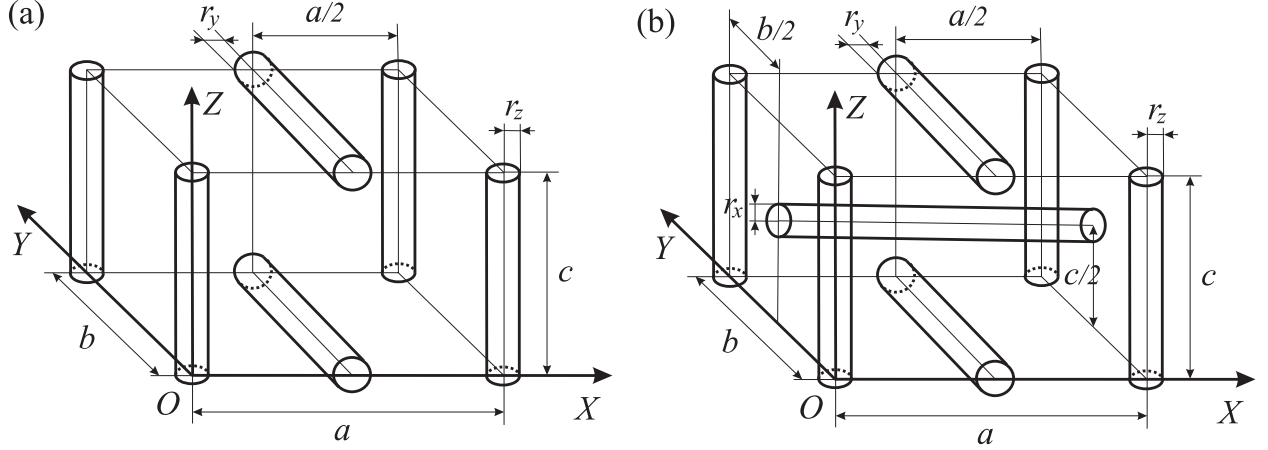


Figure 14: Elementary cells of (a) two- and (b) three-dimensional wire media [P9].

explicit dispersion equations are presented and studied. A possibility to introduce an effective permittivity is discussed. The theory is validated by comparison with numerical data available in the literature. The transmission-line modes inherent to the simple wire medium are hybridized in the case of two- and three-dimensional wire media. Typical isofrequency contours for a 2d wire medium are presented in Fig. 15. At the frequencies below the plasma

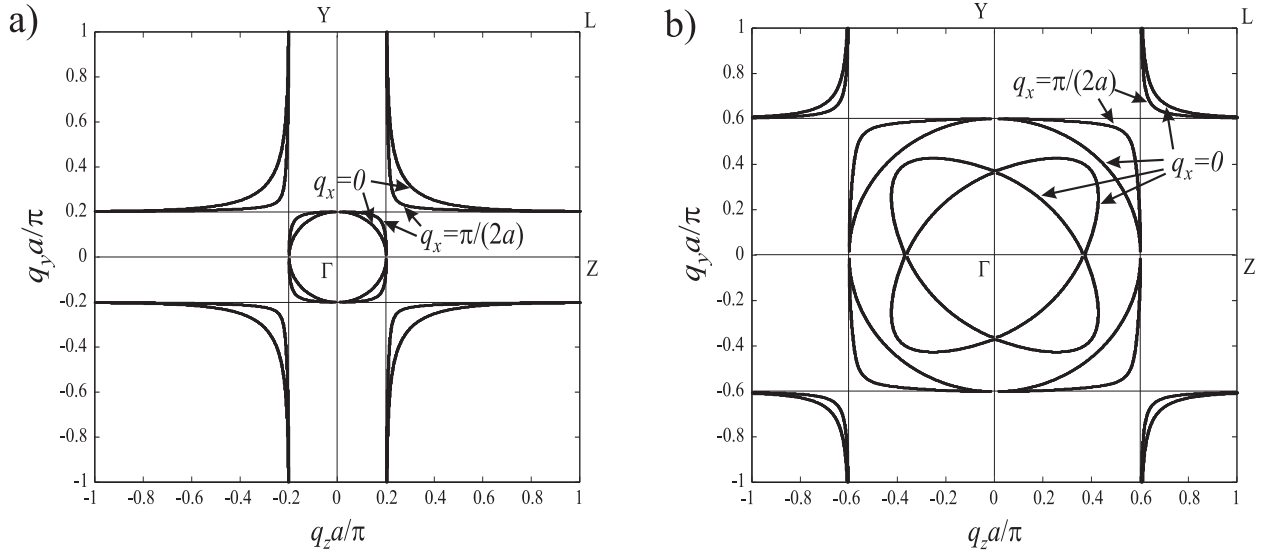


Figure 15: Isofrequency contours of a two-dimensional wire medium below (a) and above (b) the plasma frequency [P9].

frequency the medium supports hybrid transmission-line modes only. Above the plasma frequency also the modes related to the plasma-like behavior of the material appear. These modes have isofrequency contours of the form of crossing ellipses (see Fig. 15.b). All these phenomena are evidence of low-frequency spatial dispersion effects in the wire medium.

2.6 Three-dimensional electromagnetic crystals

The problem of homogenization of bulk arrays of small scatterers operating in the applied field as dipoles (electric or magnetic) has a long history. One can recall here the classical works of Lorentz, Madelung, Ewald and Oseen. However, in what concerns the homogenization of arrays of small resonant scatterers these classical results were revised in 1970-s taking into account the possible shortening the propagating wave at the resonance and the strong mutual coupling of resonant particles. It was done in the seminal work by Sipe and Kranendonk [119]. In paper [P6] such crystals are considered as electromagnetic crystals, but not as homogeneous media. The electromagnetic crystal and the typical scatterers considered in

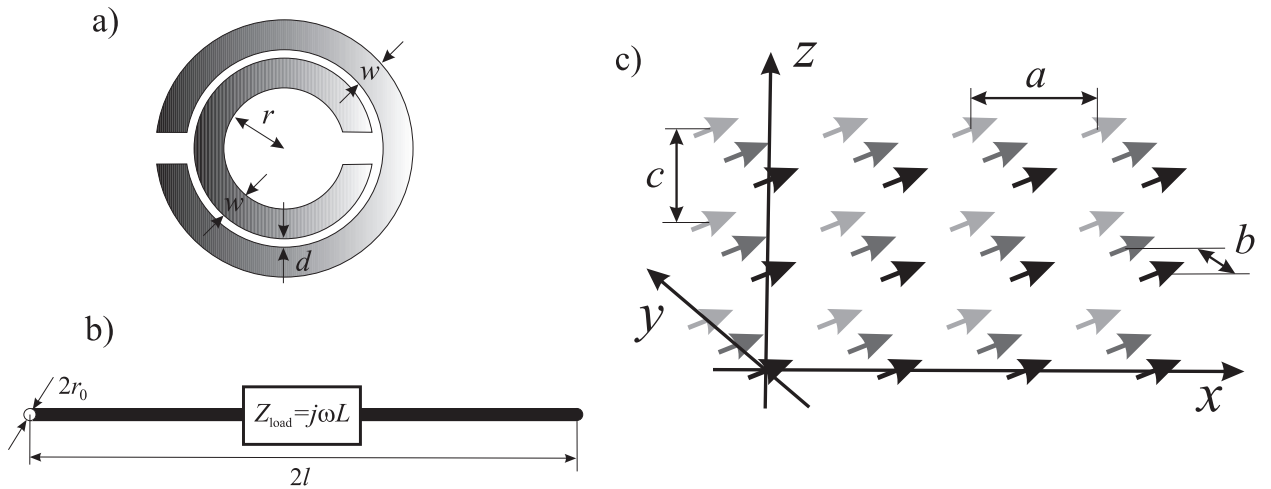


Figure 16: Typical scatterers which can be replaced by point dipoles with fixed orientation: a) split-ring resonator (magnetic dipole), b) short loaded wire (electrical dipole); and a three-dimensional electromagnetic crystal formed by the point scatterers [P6].

[P6] are presented in Fig. 16. Analytical expressions for the magnetic polarizability of split-ring resonators are available in paper [27]. The electrical polarizability of short loaded wires has been studied in detail in [P12]. An analytical dispersion theory for the three-dimensional lattice formed by point dipoles is presented in [P6]. The mathematical computations in this case happens to be much more complicated than in the cases of two-dimensional crystals considered in [P15,P17,P20]. Nevertheless, the resulting cumbersome expressions provide excellent opportunity to analyze this type of the crystals. The result of the paper [P13] was used as auxiliary one during complex calculations in [P6].

The main goal of the study in [P6] has been to determine the conditions under which the homogenization of crystals formed by resonant scatterers can be made. Therefore the consideration is limited to the frequency region where the wavelength in the host medium is larger than the lattice periods. It is demonstrated that together with the known restriction on the homogenization related with the large values of the material parameters [119] there is

an additional restriction related with their small absolute values. From the other hand, the homogenization becomes allowed in both cases of large and small material parameters for special directions of propagation. Two unusual effects inherent to the crystals under consideration are revealed: a flat isofrequency contour which allows sub-wavelength imaging using canalization regime (see the corresponding section below) and birefringence of extraordinary modes which can be used for beam splitting.

The reflection/transmission properties of the crystals under consideration have been extensively studied in [P4], where the problem of plane-wave diffraction on semi-infinite orthorhombic electromagnetic (photonic) crystals of general kind is considered. Boundary conditions are obtained in the form of an infinite system of equations relating the amplitudes of the incident wave, eigenmodes excited in the crystal and scattered spatial harmonics. Generalized Ewald-Oseen extinction principle is formulated on the base of deduced boundary conditions. The knowledge of properties of infinite crystal's eigenmodes provides an option to solve the diffraction problem for the corresponding semi-infinite crystal numerically. In the case when the crystal is formed by small inclusions which can be treated as point dipolar scatterers with a fixed direction, the problem admits complete rigorous analytical solution. The amplitudes of excited modes and scattered spatial harmonics are expressed in terms of the wave vectors of the infinite crystal by closed-form analytical formulae. The result is applied to study reflection properties of a metamaterial formed by a cubic lattice of split-ring resonators.

Electrically controllable nonreciprocal electromagnetic bandgap materials were considered in paper [P18]. A simple analytical theory of dispersion for cubic lattices of small ferrimagnetic spheres has been presented for the axial propagation along the direction of magnetization field. The dispersion equation has been solved both analytically using a kind of averaging and numerically in the exact formulation. The approximate solution leads to a very simple analytical formula for the propagation constant. Numerical calculations show that this approach has a very small mismatch with the exact one for the propagating modes. For the analysis inside the bandgap the exact solution is required, in particular near the lower boundary of the gap. The dispersion curves for the new nonreciprocal crystal have been plotted and it has been shown that this crystal has a very interesting bandgap structure. The properties of the crystal very strongly depend on polarization. For the right circular polarization a novel bandgap corresponding to the ferrimagnetic resonance is found in addition to the classical lattice bandgaps. For the left circular polarization the ferrimagnetic bandgap has not been found, as expected. The ferrimagnetic bandgap is rather wide and its central frequency is easily tunable by the magnetization field. At frequencies inside the gap the lattice period can be still very small compared to the wavelengths, which is an important feature allowing to design compact structures. The new bandgap is not complete, it exists

only for one of the two eigenpolarizations. Although the other propagation directions have not been considered, there is no reason to expect that the gap can exist for all propagation directions in this anisotropic medium.

2.7 Sub-wavelength waveguides

Recently, a very unusual waveguide was proposed by R. Marques in [20] and then extensively studied by S. Hrabar in [21]. It is a rectangular metallic waveguide periodically loaded by resonant magnetic scatterers, split-ring resonators (SRR:s), see Fig. 17. The waveguide supports a propagating mode within a frequency band near the resonance of SRR:s even if

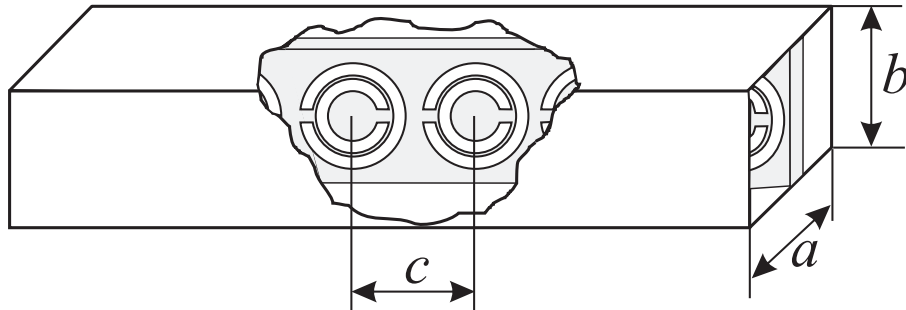


Figure 17: Sub-wavelength metallic waveguide loaded by split-ring resonators [P5].

it is located below the cutoff frequency of the hollow waveguide [20, 21]. The transversal dimensions of the waveguide happen to be much smaller than the wavelength in free space. Thus, loading by SRR:s makes the waveguide sub-wavelength and provides a method for miniaturization of guiding structures. The mode of the waveguide is a backward wave (the group and phase velocities are antiparallel). This effect was interpreted in [20] in terms of the effective double-negative media to a slab of which such waveguide is apparently equivalent.

The dispersion properties of rectangular metallic waveguides periodically loaded by uniaxial resonant scatterers are studied in [P5] with the help of an analytical theory based on the local field approach presented in [P6], the dipole approximation and the method of images. The cases of both magnetic and electric uniaxial scatterers with both longitudinal and transverse orientations with respect to the waveguide axis are considered. It is shown that in all considered cases waveguides support propagating modes below cutoff of the hollow waveguide within some frequency bands near the resonant frequency of the individual scatterers. The modes are forward ones except for the case of transversely oriented magnetic scatterers when the mode turns out to be backward. The described effects can be applied for miniaturization of guiding structures.

2.8 Double-negative materials

The first realization of double-negative media at microwave frequencies was proposed in [14] as a lattice of wires and split-ring resonators. The idea has been successfully checked experimentally in [43, 51, 70]. This structure formed by combined lattices of infinitely long wires and split-ring resonators (see Fig. 18) is studied theoretically in [P11]. A dispersion

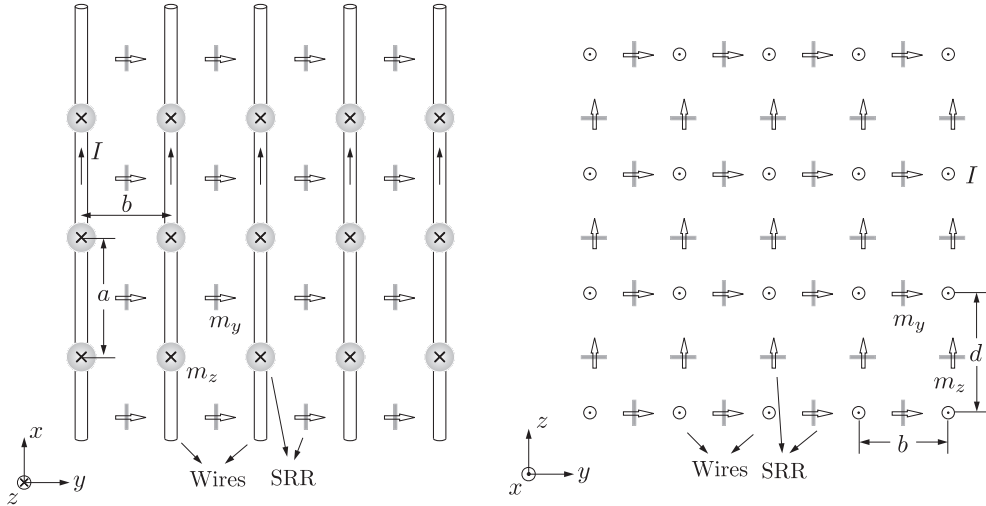


Figure 18: The lattice of split-ring resonators (shown as disks; the magnetic dipoles are indicated with arrows) and straight wires. Left: front view, right: top view [P11].

equation is derived and then used to calculate the effective permittivity and permeability in the frequency band where the lattice can be homogenized. The explicit dispersion equation clearly confirms the existence of a narrow passband within the resonant band of the split-ring resonators. In this passband the group and phase velocities of the propagating wave are in the opposite directions (i.e., it corresponds to a backward wave). Negative refraction can be explained in terms of backward waves without introducing the concept of negative material parameters. However, in the present case the homogenization turns out to be possible in the frequency range of backward waves. The obtained dispersion curves have been used to calculate the effective permittivity and permeability in the frequency band where the structure can be homogenized. It is interesting to see that the dispersion curves agree well with the Veselago theory which predicts backward waves when both permittivity and permeability are negative. Outside the resonant band of the split-ring resonators, the effective permittivity of the whole structure is the same as that of the wire lattice and the effective permeability is equal to 1. However, within the SRR resonant band, there is a sub-band where the homogenization is forbidden because a complex mode satisfies the dispersion equation at these frequencies. We found that the frequency region in which both ϵ and μ are negative coincides approximately with the backward-wave band. In this region the frequency dependence of the effective permittivity is abnormal. We interpret this as a result of the

low-frequency spatial dispersion which is inherent for the wire medium in the presence of resonant scatterers. The approximate coincidence of the backward-wave band and the band of negative material parameters confirms, in general, the concept of the structure under consideration as a uniaxial variant of Veselago media.

2.9 Backward waves and negative refraction

There is a very important question for applications: is there any possibility to achieve the effects of backward waves and/or negative refraction without using magnetic media. The backward wave and negative refraction effects can be observed in several photonic crystals [126–129] under certain circumstances. Usually these effects appear near spatial resonances (stopbands) of the structure when the characteristic period of the crystal becomes comparable with the wavelength. These new results were predicted by L.I. Mandelshtam [58] in 1940.

The property of a wave to be forward or backward is determined only by the medium properties without consideration of refraction problems. At the same time, the phenomena of positive/negative refraction and forward/backward waves with respect to the interface are determined not only by the media properties, but also by the properties of the interface. The orientation of the interface with respect to the inner geometry of the medium plays an important role here. The accurate definitions of positive/negative refraction and forward/backward waves with respect to the interface have been done in [P16], but the consideration was restricted to the case when the incident wave comes from an isotropic dielectric. The situation can be much more difficult in the case when the medium, from which the incident wave is coming, is a material of general kind [130, 131].

Note, that the group velocity $\mathbf{v}_g = \text{grad}_{\mathbf{q}}\omega$ is oriented in the same direction as the Poynting vector \mathbf{S} in passive media where the averaged stored energy U is positive, since $\mathbf{S} = U\mathbf{v}_g$ [82, 132]. From the other hand, in active and non-equilibrium media [133, 134] it is possible to meet the situation when the averaged stored energy is negative, and thus the group velocity and the Poynting vector are oriented in the opposite directions.

Negative refraction and backward waves have different applications, in which sometimes not both of these effects are required together. Pendry in [40] used the negative refraction effect for focusing, and the backward-wave effect to have all incoming rays in phase, but the last goal can be achieved using forward waves also [135]. Engheta in [52] used the property of a wave to be backward with respect to the interface. Negative refraction and backward-wave effects are inherent to double-negative media, but both of these effects can be observed in other materials as well. For example, it is enough for the media to be a uniaxial dielectric,

and this fact provides a possibility to observe negative refraction [136, 137]. In this case the negative refraction happens when the refracted wave is forward (in both general meaning and with respect to the interface).

An overview of results related to negative refraction and backward-wave effects in electromagnetic and photonic crystals is available in [P10] and [138, 139]. A possibility to observe negative refraction and backward wave with respect to the interface in uniaxial dielectrics with negative permittivity along the anisotropy axis is discussed in [P16].

3 Sub-wavelength imaging using canalization regime

3.1 Preamble

Resolution of common imaging systems is restricted by the so-called diffraction limit, since they operate only with propagating spatial harmonics emitted by the source. Conventional lenses cannot transmit evanescent harmonics which carry sub-wavelength information, since these waves exhibit exponential decay in usual naturally occurring materials. In order to overcome the diffraction limit it is required to use another sort of materials for the construction of lenses. It is required to engineer an artificial material (metamaterial) with electromagnetic properties which dramatically differ from those of materials available in nature [140]. The theoretical possibility of sub-wavelength imaging by a slab of double-negative medium with $\epsilon = \mu = -1$ was demonstrated by J. Pendry in his seminal work [40]. The focusing phenomenon in Pendry's perfect lens is based on two effects. The propagating modes of a source are focused due to the negative refraction and the evanescent modes experience amplification inside the DNG slab (see Fig. 19). This allows to restore sub-wavelength details in the focal plane. The second effect happens due to the resonant excitation of sur-

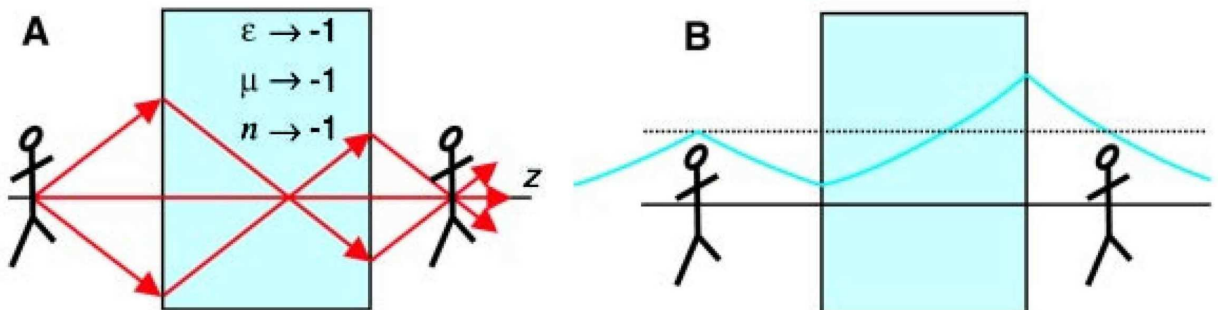


Figure 19: Sub-wavelength imaging by perfect lens formed by double-negative material: a) ray tracing corresponding to focusing of propagating modes (far-field), b) amplification of evanescent modes (near-field) [140].

face plasmons at the interfaces of the slab. This resonant excitation is inherent not only to the slabs of DNG: similar effects are observed for a pair of resonant grids or conjugating planes [141, 142].

The promising theoretical predictions meet numerous practical difficulties in the creation of double-negative metamaterials. On one hand, the major problem is the creation of materials possessing magnetic properties at optical and terahertz frequencies [71, 72]. On the other hand, the issues related to losses play a very important role as well. Numerous problems are closely related with fundamental restrictions and can be hardly overcome. It is an ambitious goal to obtain sub-wavelength resolution without DNG in the optical frequency range. In this range the negative refraction phenomenon is observed in photonic crystals at the frequencies close to the bandgap edges. This fact was theoretically revealed by M. Notomi [128], confirmed by other authors [50, 143] and experimentally verified by P.V. Parimi et al. [144]. The fact that photonic crystals in certain regimes possess similar to double-negative media properties [145] makes such materials quite prospective for the design of flat sub-wavelength lenses. A flat *superlens* formed by a slab of photonic crystal was suggested by C. Luo et al. in [135] and a possibility of sub-wavelength imaging was theoretically studied in [146]. An experimental verification of the imaging effect was demonstrated in [147]. The principle of Luo's superlens is similar to the principle of Pendry's perfect lens: negative refraction for propagating modes and amplification due to resonant surface plasmons for evanescent modes. Both effects are obtained without double-negative properties of a material. Negative refraction is obtained due to a specific form of isofrequency contours (without backward waves inherent to DNG). Further increase of the resolution for Luo's superlens can be achieved by simultaneously increasing the dielectric permittivity of the host medium and decreasing the lattice period [146]. In practice, this is not a helpful way in the optical frequency region where large permittivity for real media is related with high losses. Also, an important factor deteriorating the image is a finite thickness of the superlens. The eigenmodes excited in the crystal experience multiple reflections from the interfaces and their interference disturbs the image. This destructive interference appears due to a mismatch between the wave impedances of air and photonic crystal, and is inevitable for some angles of incidence. In the case of Pendry's perfect lens this defect is avoided because the double-negative medium with $\varepsilon = \mu = -1$ is matched with air for all angles of incidence. C. Luo et al. in [135] partially solved the problem of matching by choosing an appropriate thickness of the slab. In this case the slab operates as a Fabry-Perot resonator. However, this solution is not complete since the Fabry-Perot resonance holds only for a narrow range of incidence angles.

At the present time, there are two types of regimes which are used for sub-wavelength imaging using photonic crystals. The both regimes are based on the use of isofrequency contours

shrinking with growing frequency and providing negative refraction. In the first case the isofrequency contours shrink around corner points of the first Brillouin zone [135, 146–152]. This regime is observed at frequencies near the bottom edge of the first bandgap. In the second case the isofrequency contours shrink around the central point of the first Brillouin zone [148, 153–157] which makes this case completely similar to DNG. This regime is usually observed at frequencies near the bottom edge of the second bandgap, but it can be achieved at the higher bands [158, 159] as well.

3.2 Canalization regime in a slab of capacitively loaded wire medium

A different regime of sub-wavelength imaging than in [40, 135] has been proposed in [P8]. This regime does not involve negative refraction and amplification of evanescent modes. The concept is to transform most part of the spatial spectrum of the source radiation into propagating eigenmodes of the crystal having practically the same group velocity (directed across the slab) and the same longitudinal components of the wave vector (see Fig. 20). Spatial harmonics produced by a source (propagating and evanescent) refract into the crystal eigenmodes at the front interface. These eigenmodes propagate normally to the interface and deliver the distribution of near-field electric field from the front interface to the back interface without any disturbances. This way the incident field with sub-wavelength details is transported from one interface to the other one. The described regime was called in [P8] as *canalization*.

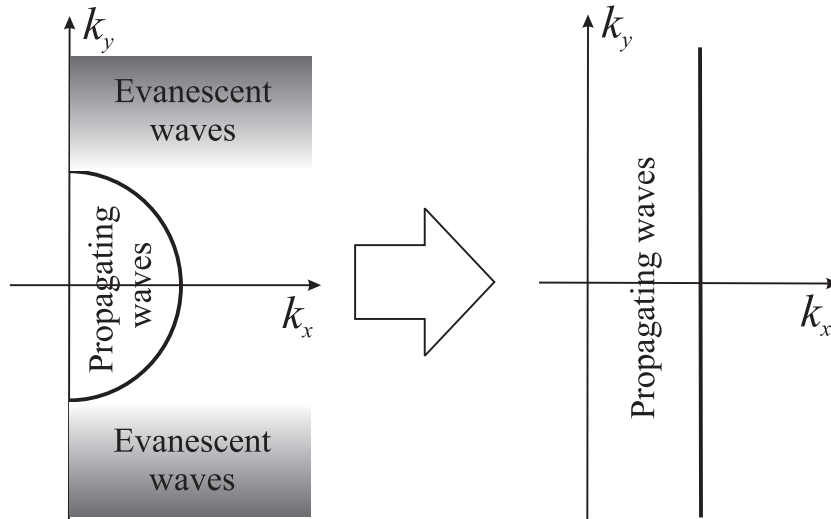


Figure 20: Illustration of canalization principle of sub-wavelength imaging.

Similar regimes for propagating spatial harmonics are called as self-guiding [160], directed diffraction [161], self collimation [162–164] and tunneling [165]. One can see from the results of papers [161, 163, 165] that canalization dominates over negative refraction in the superlens

suggested in [135]. However, in these papers canalization for evanescent harmonics was not noticed. It allows us to avoid negative refraction at all while obtaining a superlens and achieve sub-wavelength resolution. In fact, canalization has a similar principle of operation as a medium with zero refraction index [166]. The difference is that in our case the image is transmitted by waves which all vary identically with the distance from the front interface, whereas in a zero refraction index medium there is no such variation. Also, a similar effect has been observed in bilayers of media with indefinite permittivity and permeability tensors [77] where a pair of layers, effectively compensating the properties of each other, provides total transmission within a wide range of transverse wave vectors.

The problem of strong reflection from a slab can be solved by choosing its thickness appropriately so that it operates as a Fabry-Perot resonator. In our case the Fabry-Perot resonance holds for all incidence angles and even for incident evanescent waves. The reason is that after the refraction all these waves acquire the same longitudinal component of the wave vector for which the Fabry-Perot resonator is tuned. Thus, in the canalization regime the superlens does not suffer an image deterioration due to its finite width. Moreover, the proposed regime helps to avoid the problems related to finite transverse size of the lenses (inherent to DNG slabs [167]), because there are no waves traveling along the interfaces.

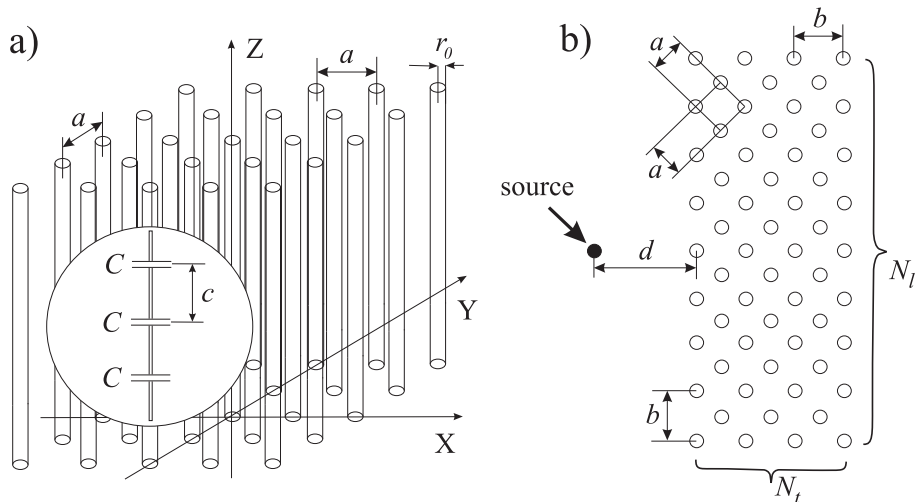


Figure 21: a) Capacitively loaded wire medium and b) lens formed by CLWM [P8].

The canalization regime can be implemented by using an isofrequency contour which has a rather long flat part. Such contours are available for different types of photonic and electromagnetic crystals. For example, the capacitively loaded wire medium (CLWM) has flat isofrequency contours at frequencies close to the lower edge of the resonant bandgap [P8]. The CLWM was chosen in [P8] since the analytical result for the dispersion properties of the infinite CLWM is available in [P17], and the finite size samples of CLWM with large number of loaded wires can be easily numerically analyzed [168]. The CLWM has a bandgap near the resonant frequency of a single capacitively loaded wire, the so-called *resonant bandgap*, which

can be tuned by changing the value of the load capacitance. A high value of capacitance allows us to locate the resonant bandgap at much lower frequencies than the first lattice resonance [P17]. This way it is possible to obtain a bandgap at very low frequencies without increasing the dielectric permittivity of the host medium. Note, that this resonant bandgap has the same nature as the bandgap caused by resonant properties of a component material as in [120] or [P18].

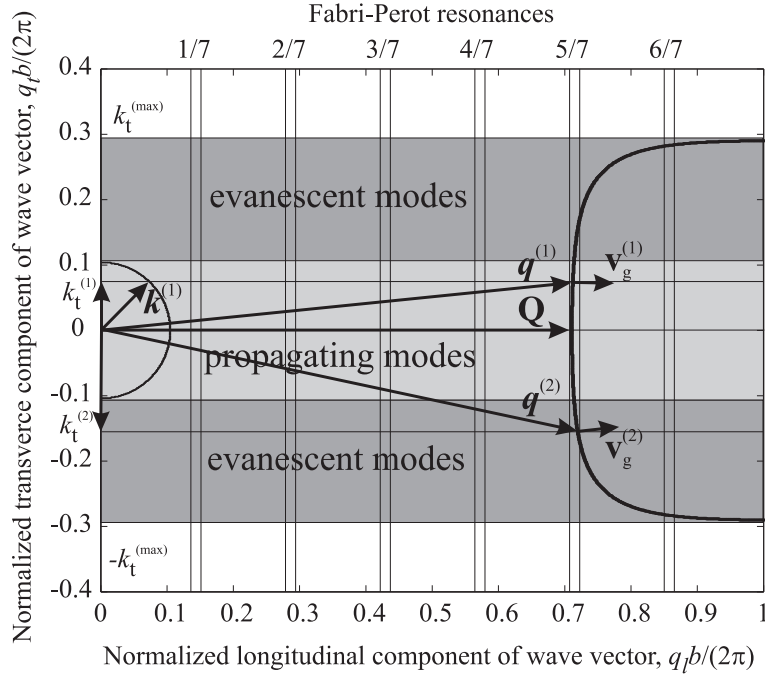


Figure 22: Isofrequency contours for the canalization regime [P8].

The isofrequency contours for the canalization regime in CLWM slab are shown in Fig. 22. The circle at the left side of Fig. 22 is the isofrequency contour of the host medium and the curve at the right side is the CLWM isofrequency contour. All propagating spatial harmonics of a source and a wide range of evanescent ones refract into eigenmodes with the longitudinal wave vector close to \mathbf{Q} . There is a part of the isofrequency contour with $|k_t| \approx k_t^{\max}$ which is not flat but it corresponds to a very narrow band of evanescent wave spectrum and we neglect its contribution. The light shaded region ($|k_t| \leq k$) in Fig. 22 corresponds to propagating incident waves. The dark shaded regions ($k < |k_t| \leq k_t^{\max}$) correspond to the evanescent incident waves which transform into propagating eigenmodes after refraction. Refraction of the propagating wave with $k_t = k_t^{(1)}$, $|k_t^{(1)}| < k$ and the evanescent wave with $k_t = k_t^{(2)}$, $k < |k_t^{(2)}| \leq k_t^{\max}$ is illustrated in Fig. 22. Both waves refract (keeping the transverse wave vector component) into eigenmodes which have longitudinal wave vectors close to \mathbf{Q} and practically identical group velocities ($\mathbf{v}_g^{(1)}$ and $\mathbf{v}_g^{(2)}$) directed across the slab. Though the transversal components of the wave vector are retained in the refraction ($q_t = k_t$), this does not mean the transversal propagation of refracted power

(similar to the transmission-line modes of wire media [P15])! These components describe the transversal distribution of the field traveling across the slab.

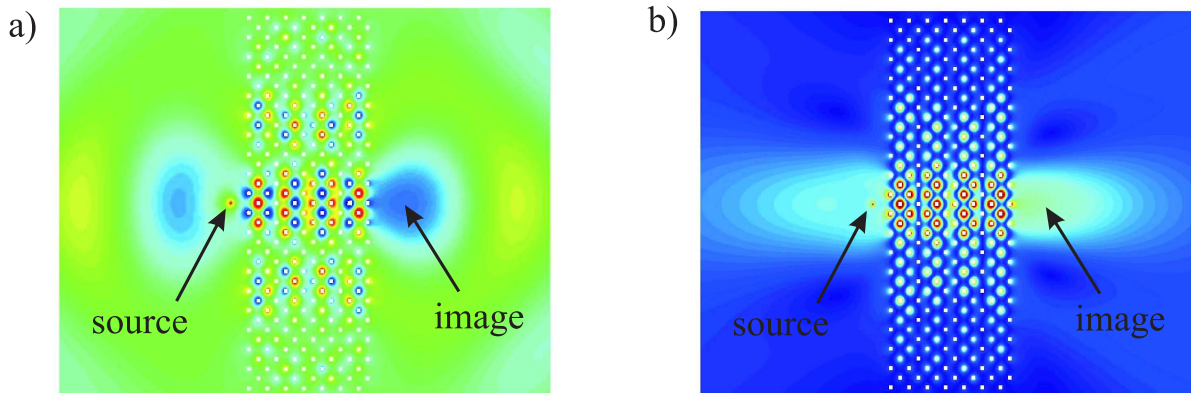


Figure 23: Distribution of electric field amplitude (a) and intensity (b) for the sub-wavelength lens formed by a capacitively loaded wire medium operating in the canalization regime [P8].

The result of numerical simulation for the excitation of a CLWM slab by a point source (from [P8]) is presented in Fig. 23. An image near the back interface is observed. The radius of the focal spot is approximately $\lambda/6$, which means that a sub-wavelength resolution is observed and that the canalization allows transportation of a sub-wavelength images from one interface to the other. An experimental verification of sub-wavelength imaging using CLWM slabs has been done in [P3] and resolution of $\lambda/10$ has been demonstrated. Though imaging can be achieved only with the sources which are located enough close to the front interface, the utilization of the canalization regime is advantageous as compared to Pendry's perfect lens. The lens can be made thick, since its required thickness is not related with the distance to the source. It is practically important for the near-field microscopy in the optical range, when the needle of a microscope used as a probe can be located physically far from the tested source. Then one can use a mechanically solid superlens in order to avoid destruction of objects under test by the microscope.

3.3 Lens formed by a wire medium for microwave frequencies

The canalization regime offers an attractive possibility for transportation of sub-wavelength images. The main requirement for that purpose is flatness of some part of an isofrequency contour. In [P8] it has been demonstrated that such contours are available for CLWM at microwaves. The CLWM slab operates as an imaging device only for s -polarized incident waves. For p -polarized waves there is another possibility to obtain a flat isofrequency contour in a material. A perfectly flat and infinitely long isofrequency contour corresponds to transmission-lines in wire medium. The imaging device formed by an array of parallel

conducting wires (a slab of wire medium) studied in [P2] is presented in Fig. 24. At the first sight it seems that this structure is an electrical analogue of Wiltshire's system [169, 170]. An array of Swiss rolls, being similar to magnetic wires, is capable to transmit s -polarized (transverse electric, TE) spatial harmonics of the source spectrum. An array of wires operates in the same manner, but for p -polarized (transverse magnetic, TM) waves. In other

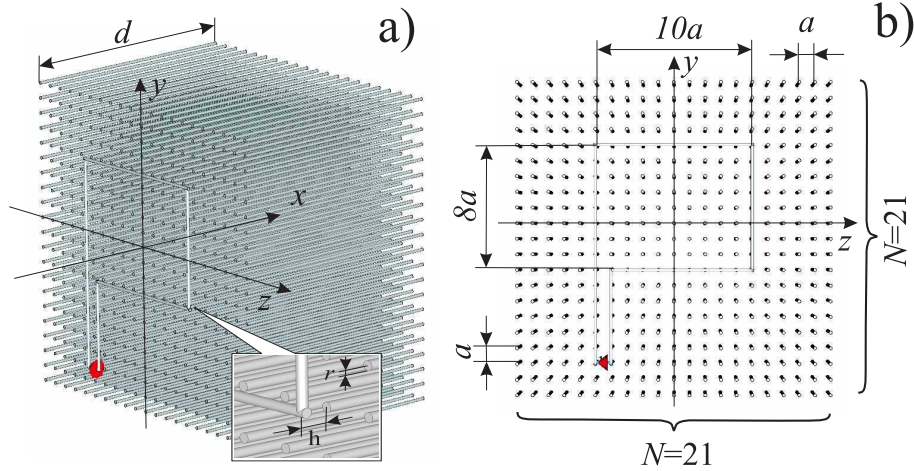


Figure 24: Geometry of a flat lens formed by a wire medium and a source of the form of letter P: a) perspective view, b) front view [P2]. $a = 10$ mm, $r = 1$ mm, $d = 150$ mm, $h = 5$ mm, $f = 1$ GHz.

words, an array of Swiss rolls restores at the back interface the normal component of the magnetic field produced by a source. An array of wires restores the normal component of electric field. At the same time, there is a serious difference between Wiltshire's system and a slab of wire medium. Swiss rolls are artificial resonant structures which behave as magnetic wires only at frequencies in the vicinity of the resonance. This fact preconditions Swiss rolls to be narrow-band and very lossy. Conducting wires in this sense are natural electrical wires. It means that they are wide-band and practically lossless. The absence of strong losses (inherent in Swiss rolls) in ordinary wires lifts restriction on the lens thickness. It allows us to create sub-wavelength lenses of nearly arbitrary thickness and deliver images with sub-wavelength resolution into far-field region of the source and beyond [P7]. The imaging system effectively works as a telephone exchange [171] formed by multi-conductor transmission line.

Numerical simulations of the structure presented in Fig. 24 were performed in [P2] using CST Microwave Studio package. The lens consisting of 21×21 array of aluminium wires excited by a source in the form of letter P was modelled. The working frequency f is 1 GHz, the length of wires (the thickness of slab) d is 15 cm (half of the wavelength), the period of lattice a is 1 cm, the radius of wires r is 1 mm. The source is placed at $h = 5$ mm distance from the front interface of the lens and fed by a point current source $I = 1$ A. The results of simulation are presented in Fig. 25. The source produces a sub-wavelength distribution of

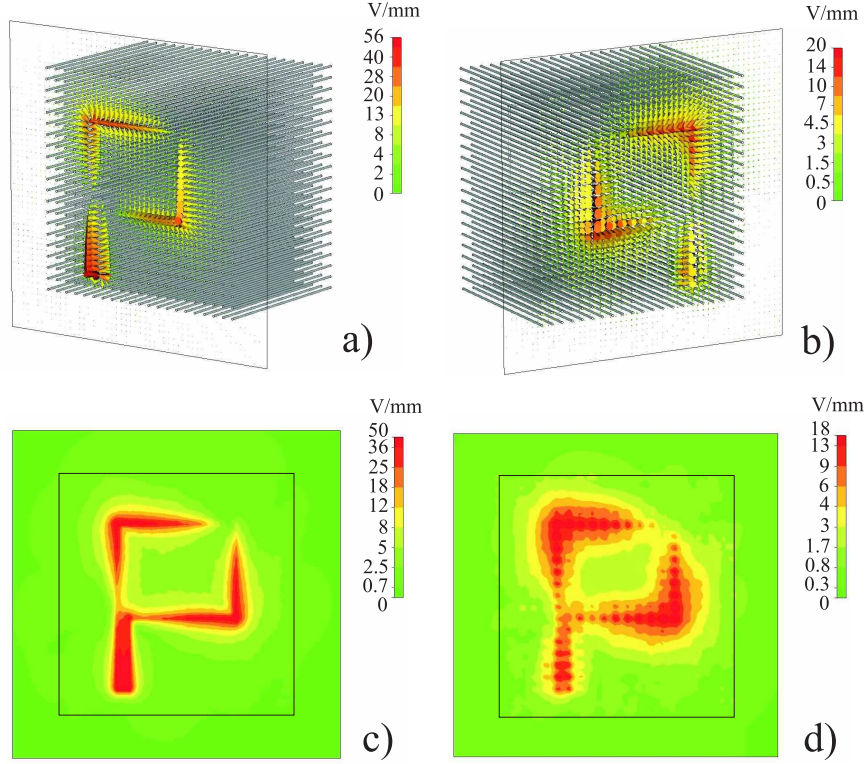


Figure 25: Distribution of electric field and its absolute value: (a), (c) at 2.5mm distance from the front interface; (b), (d) at 2.5mm distance from the back interface [P2].

electrical field at the front interface of the slab, see Fig. 25.a. The p -polarized contribution of the field is canalized from the front interface to the back interface and forms an image, see Fig. 25.b. The quality of the image can be clearly seen in Fig. 25.c and d, where absolute values of electrical field in vicinity of the front and back interfaces are plotted. The local maxima of intensity produced by terminations of the wires are visible in Fig. 25.d. The resolution of imaging in the present case is equal to 2 cm (double period of the structure), which is one fifteenth of the wavelength ($\lambda/15$). The slab of wire media with parameters as in Fig. 24 was constructed and experimental verification of the sub-wavelength imaging with $\lambda/15$ resolution was confirmed in [P2].

The present realization of canalization regime with the help of wire medium is advantageous at microwave frequencies, but it can not be realized in optics, where metals behave as dielectrics with negative permittivity. It does not mean that implementation of canalization regime in optical range is impossible. This regime can be realized using photonic crystals [135,147], but resolution of such lenses will be restricted by the period of crystals [146] which cannot be reduced too much due to absence of high-contrast lossless materials at the optical range. Another possibility is to construct a uniaxial material with infinite permittivity along the anisotropy axis. It can be done using lattices of resonant uniaxial nanoparticles or multilayered structures [171,172].

3.4 Metal-dielectric layered structure for optical frequencies

A lens formed by the wire medium is a unique sub-wavelength imaging device for microwave frequencies where metals are nearly ideally conducting. At higher frequencies including the visible range such a lens will not operate properly since metals at these frequencies have plasma-like behavior. In paper [P1] a different structure which can operate in the canalization regime in the optical frequency range is proposed. This is a sub-wavelength optical “telegraph” which operates completely on the same principle as a slab of wire medium at microwaves. For the transmission-line modes the component of effective permittivity of wire medium (1) corresponding to the direction along the wires becomes infinite. In order to achieve in the optical range the same properties as the wire medium has at microwave frequencies it is required to find some uniaxial optical material which has infinite permittivity along the anisotropy axis. Usually, it is assumed that in the optical range it is impossible to get very high values of permittivity. It is true for natural materials, but for metamaterials, especially uniaxial, it is not so. A high permittivity can be achieved in layered metal-dielectric structures [171–174].

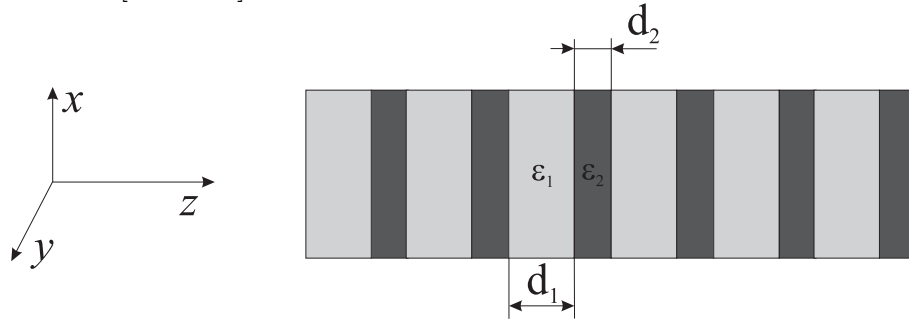


Figure 26: Geometry of layered metal-dielectric metamaterial [P1].

At the long-wavelength limit ($d_1, d_2 \ll \lambda$) a layered structure presented in Fig. 26 can be described by the permittivity tensor of the form:

$$\bar{\bar{\epsilon}} = \epsilon_{\parallel}(\mathbf{xx} + \mathbf{yy}) + \epsilon_{\perp}\mathbf{zz}, \quad (6)$$

where

$$\epsilon_{\parallel} = \frac{\epsilon_1 d_1 + \epsilon_2 d_2}{d_1 + d_2}, \quad \epsilon_{\perp} = \left[\frac{\epsilon_1^{-1} d_1 + \epsilon_2^{-1} d_2}{d_1 + d_2} \right]^{-1}.$$

In order to get $\epsilon_{\parallel} = 1$ and $\epsilon_{\perp} = \infty$, required for implementation of the canalization regime, it is necessary to choose parameters of the layered material so that $\epsilon_1/\epsilon_2 = -d_1/d_2$ and $\epsilon_1 + \epsilon_2 = 1$. From the first equation it is clear that one of the layers should have negative permittivity and thus, the structure has to be formed by one dielectric layer and one metallic layer. For example, one can choose $\epsilon_1 = 2$, $\epsilon_2 = -1$ and $d_1/d_2 = 2$, or $\epsilon_1 = 15$, $\epsilon_2 = -14$ and $d_1/d_2 = 15/14$.

Note, that no layered structure required for canalization regime can be formed using equally thick layers $d_1 = d_2$. The layered metal-dielectric structures considered in [171,172,174] have completely different properties as compared to the structures considered in paper [P1]. As it is noted in [172], the structures with $d_1 = d_2$ and $\epsilon_1 = -\epsilon_2$ (as in [171,172,174]) correspond to $\epsilon_{\perp} = 0$ and $\epsilon_{\parallel} = \infty$, and operates as an array of wires embedded into a medium with zero permittivity. Such a structure can be considered as an unmatched uniaxial analogue of so-called material with zero-index of refraction [166]. Absence of matching ($\mu = 1$, but not 0, as it is required) causes strong reflections and restricts the slab thickness to be thin. In contrast to this case, in the canalization regime the reflections from the slab are absent due to the Fabry-Perot condition which holds for all angles of incidence.

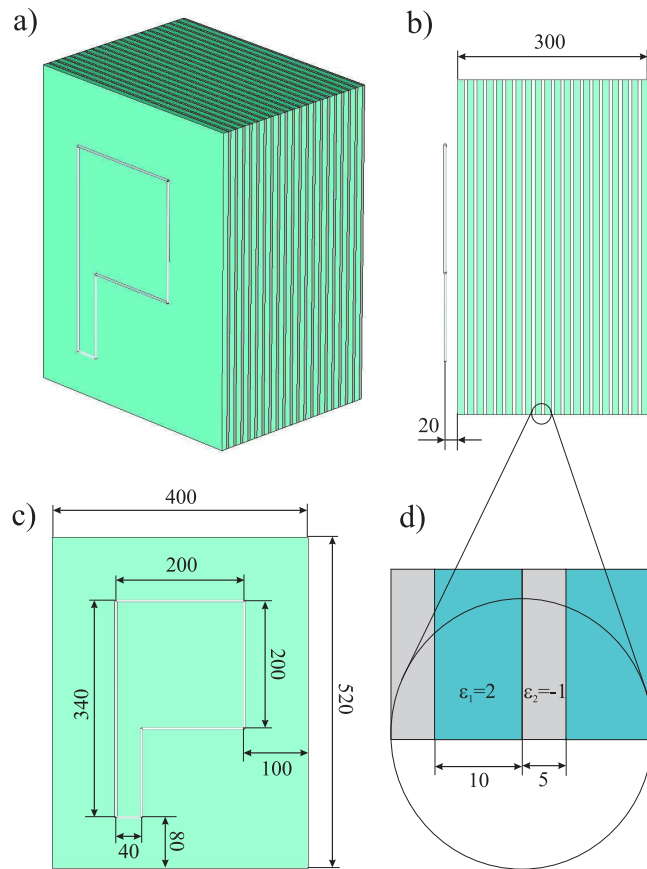


Figure 27: Geometry of flat lens formed by a layered metal-dielectric metamaterial [P1]: a) perspective view, b) side view, c) front view, d) small details. All dimensions are in nm.

In order to demonstrate how the canalization regime can be implemented using the suggested metal-dielectric layered structure, numerical simulations using the CST Microwave Studio package have been done in [P1]. A sub-wavelength source (a loop of current in the form of P-letter) is placed at 20 nm distance from a 300 nm thick multi-layer slab composed of 10 nm and 5 nm thick layers with $\epsilon_1 = 2$ and $\epsilon_2 = -1$, respectively. The detailed geometry of the structure is presented in Fig. 27. The wavelength of operation λ is 600 nm. The

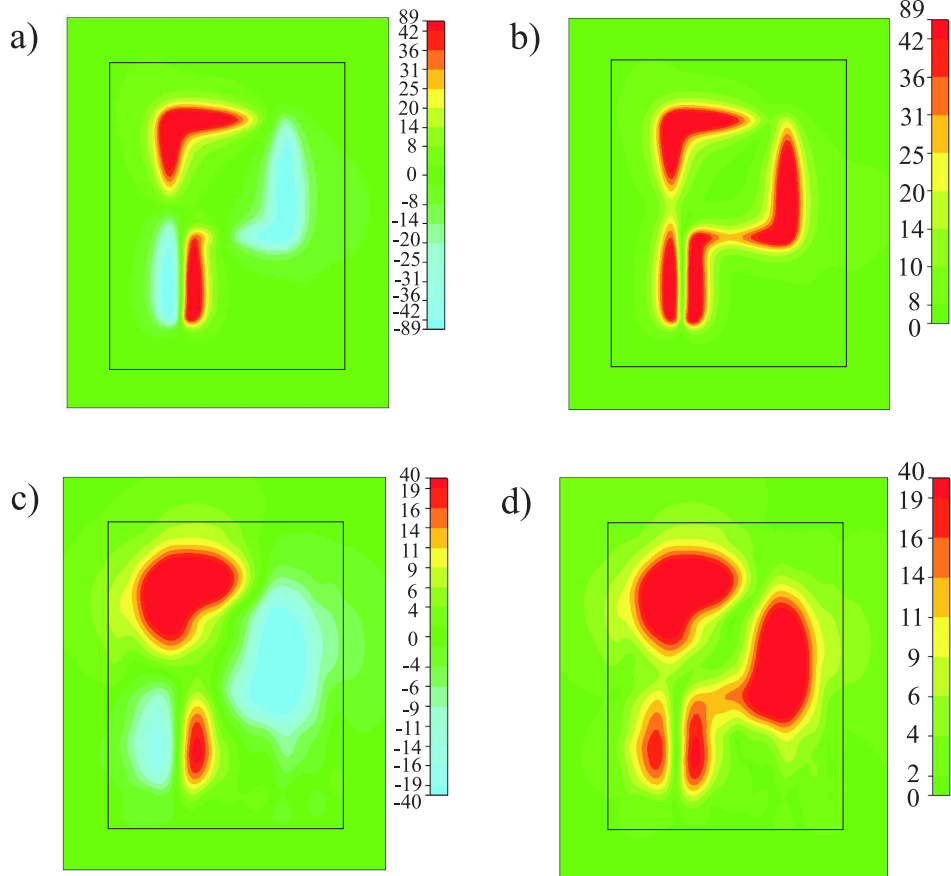


Figure 28: Distributions of the normal to the interface component of electric field at 20 nm distances: a) from the source, c) from the back interface; and their absolute values, b) and d), respectively [P1].

field distributions in the planes parallel to the interface of the lens plotted in Fig. 28 clearly demonstrate imaging with 30 nm resolution ($\lambda/20$). Figs. 28.a,b show the field produced by the source in free space at 20 nm distance. It is practically identical to the field observed at the front interface of the lens (see [P1]), which confirms that reflections from the front interface are negligibly small. Actually, the main contribution into reflected field comes from diffraction at the corners and wedges of the lens. The image at the back interface of the lens is a little bit distorted by plasmon-polariton modes excited at the back interface (see [P1]), but this distortion disappears at 20 nm distance from the back interface as it is clearly seen in Figs. 28.c,d.

The lens works in the canalization regime as a transmission device and does not involve negative refraction and amplification of evanescent modes. A material with $\epsilon = -1$ at 600 nm wavelength can be created by doping some lossless dielectric by a small concentration of silver which has $\epsilon = -15$ at such frequencies, in a similar manner to the ideas of works [175] or [176]. Even more promising resolution of $\lambda/60 = 10$ nm was predicted for a layered structure comprising 7.76 nm layers of a dielectric with $\epsilon = 15$ and 7.24 nm layers of a metal

with $\varepsilon = -14$. The last structure can be constructed using silicon as a dielectric and silver as a metal, but very accurate fabrication with error no more than 0.05 nm will be required in order to get proper result. The losses in silver in both cases are already reduced by operating at rather long wavelength of 600 nm, but in accordance with our estimations they are still high enough to destroy the quality of the sub-wavelength resolution. This problem can be solved by using active materials, for example doped silicon [172, 175]. Creation of the lens operating in canalization regime in the optical frequency range will lead to a breakthrough in manufacturing of optical drives (DVD) whose capacity at the present time is restricted by the diffraction limit.

References

- [1] W. Kock, “Metallic delay lenses,” *Bell Syst. Tech. J.*, vol. 27, pp. 58–82, 1948.
- [2] R. Collin, *Field Theory of Guided Waves*. IEEE Press, Piscataway, NJ, 1990.
- [3] A. Sihvola, *Electromagnetic mixing formulas and applications*. IEE Publishing, Electromagnetic Wave Series, London, 1999.
- [4] J. Brown, “Artificial dielectrics,” *Progress in dielectrics*, vol. 2, pp. 195–225, 1960.
- [5] J. Brown, “Artificial dielectrics having refractive indices less than unity,” *Proc. IEEE*, vol. 100, no. 62R, pp. 51–62, 1953.
- [6] J. Brown and W. Jackson, “The properties of artificial dielectrics at centimeter wavelengths,” *Proc. IEEE*, vol. 102B, no. 1699R, pp. 11–21, 1955.
- [7] J. S. Seeley and J. Brown, “The use of artificial dielectrics in a beam scanning prism,” *Proc. IEEE*, vol. 105C, no. 2735R, pp. 93–102, 1958.
- [8] A. Carne and J. Brown, “Theory of reflections from the rodded-type artificial dielectrics,” *Proc. IEEE*, vol. 105C, no. 2742R, pp. 107–115, 1958.
- [9] A. M. Model, “Propagation of plane electromagnetic waves in a space which is filled with plane parallel grids,” *Radiotekhnika*, vol. 10, pp. 52–57, 1955.
- [10] W. Rotman, “Plasma simulations by artificial dielectrics and parallel-plate media,” *IRE Trans. Ant. Propag.*, vol. 10, pp. 82–95, 1962.
- [11] J. Pendry, A. Holden, W. Steward, and I. Youngs, “Extremely low frequency plasmons in metallic mesostructures,” *Phys. Rev. Lett.*, vol. 76, no. 25, pp. 4773–4776, 1996.
- [12] A. Pokrovsky and A. Efros, “Electrodynamics of metallic photonic crystals and the problem of left-handed materials,” *Phys. Rev. Lett.*, vol. 89, p. 093901, 2002.
- [13] A. Pokrovsky, “Analytical and numerical studies of wire-mesh metallic photonic crystals,” *Phys. Rev. B*, vol. 69, p. 195108, 2004.
- [14] D. R. Smith, W. J. Padilla, D. C. Vier, S. C. Nemat-Nasser, and S. Schultz, “Composite medium with simultaneously negative permeability and permittivity,” *Phys. Rev. Lett.*, vol. 84, no. 18, pp. 4184–4187, 2000.
- [15] R. King, D. Thiel, and K. Park, “The synthesis of surface reactance using an artificial dielectric,” *IEEE Trans. Antennas and Propagat.*, vol. 31, pp. 471–476, 1983.

- [16] J. Pendry, A. Holden, D. Robbins, and W. Stewart, "Magnetism from conductors and enhanced nonlinear phenomena," *IEEE Trans. Microwave Theory Techn.*, vol. 47, no. 11, pp. 195–225, 1999.
- [17] S. Schelkunoff and H. Friis, *Antennas: Theory and practice*. New York: John Wiley and Sons, 1952.
- [18] H. Schneider and P. Dullenkopf, "Slotted tube resonator: A new nmr probe head at high observing frequencies," *Rev. Sci. Instrum.*, vol. 48, no. 1, pp. 68–73, 1977.
- [19] W. Hardy and L. Whitehead, "Split-ring resonator for use in magnetic resonance from 200-2000 MHz," *Rev. Sci. Instrum.*, vol. 52, no. 2, pp. 213–216, 1981.
- [20] R. Marques, J. Martel, F. Mesa, and F. Medina, "Left-handed-media simulation and transmission of em waves in subwavelength split-ring-resonator-loaded metallic waveguides," *Phys. Rev. Lett.*, vol. 89, no. 18, p. 183901, 2002.
- [21] S. Hrbar, J. Bartolic, and Z. Sipus, "Waveguide miniaturization using negative permeability material," *IEEE Trans. Antennas Propagat.*, vol. 53, no. 1, pp. 110–119, 2005.
- [22] A. Serdyukov, I. Semchenko, S. Tretyakov, and A. Sihvola, *Electromagnetics of bianisotropic materials: theory and applications*. Gordon and Breach Science Publishers, Amsterdam, 2001.
- [23] I. Lindell, A. Sihvola, S. Tretyakov, and A. Viitanen, *Electromagnetic Waves in Chiral and Bi-Isotropic Media*. Artech House Publishers, Boston, MA, 1994.
- [24] A. Priou, A. Sihvola, S. Tretyakov, and A. Vinogradov, *Advances in complex electromagnetic materials*. NATO ASI Series, Kluwer, 1997.
- [25] *Bianisotropic and bi-isotropic media and applications, Progress in Electromagnetic Research, PIER*, vol. 9, 1994.
- [26] R. Marques, F. Medina, and R. Rafii-El-Idrissi, "Role of bianisotropy in negative permeability and left-handed metamaterials," *Phys. Rev. B*, vol. 65, p. 144440, 2002.
- [27] B. Sauviac, C. Simovski, and S. Tretyakov, "Double split-ring resonators: analytical modeling and numerical simulations," *Electromagnetics*, vol. 24, no. 5, pp. 317–338, 2004.
- [28] S. Tretyakov, "Research on negative refraction and backward-wave media: A historical perspective," *Proc. of EPFL Latsis Symposium 2005, Negative Refraction: Revisiting Electromagnetics from Microwave to Optics, Lausanne, Switzerland, February 28-March 2*, pp. 30–35, 2005.

- [29] S. Tretyakov, I. Nefedov, A. Sihvola, S. Maslovski, and C. Simovski, “Waves and energy in chiral nihility,” *J. Electromagnetic Waves Applic.*, vol. 17, no. 5, pp. 695–706, 2003.
- [30] J. Pendry, “A chiral route to negative refraction,” *Science*, vol. 306, pp. 1353–1355, 2004.
- [31] C. Monzon and D. W. Forester, “Negative refraction and focusing of circularly polarized waves in optically active media,” *Phys. Rev. Lett.*, vol. 95, p. 123904, 2005.
- [32] C. Simovski, M. Kondratjev, P. Belov, and S. Tretyakov, “Interaction effects in two-dimensional bianisotropic arrays,” *IEEE Trans. Antennas Propagat.*, vol. 47, no. 9, pp. 1429–1439, 1999.
- [33] C. Simovski, P. Belov, and M. Kondratjev, “Electromagnetic interaction of chiral particles in three dimensional arrays,” *J. Electromagnetic Waves Applic.*, vol. 13, pp. 189–203, 1999.
- [34] P. Belov, C. Simovski, M. Kondratjev, and D. Bulgin, “Excitation of diffraction grid of bianisotropic particles by plane electromagnetic wave,” *Izvestija Vuzov, Priborostrojenije*, vol. 41, no. 3, pp. 21–32, 1998.
- [35] C. Simovski, P. Belov, and M. Kondratjev, “Excitation of multilayered grids of bianisotropic particles by plane wave,” *SPIE Proc.*, vol. 3323, pp. 691–698, 1998.
- [36] M. Kondratjev, C. Simovski, and P. Belov, “Reflection and transmission of plane waves in bianisotropic planar grids,” *SPIE Proc.*, vol. 3323, pp. 669–678, 1998.
- [37] P. Belov, C. Simovski, and M. Kondratjev, “Analytical-numerical study of electromagnetic interaction in two-dimensional bianisotropic arrays,” *SPIE Proc.*, vol. 3323, pp. 679–690, 1998.
- [38] P. Belov, C. Simovski, and M. Kondratjev, “Problem of the local field for plane grids with bianisotropic particles,” *SPIE Proc.*, vol. 3039, pp. 680–691, 1997.
- [39] C. Simovski, M. Kondratjev, P. Belov, and S. Tretyakov, “Excitation dyadics for the grids of chiral and omega particles,” *SPIE Proc.*, vol. 3039, pp. 692–703, 1997.
- [40] J. Pendry, “Negative refraction index makes perfect lens,” *Phys. Rev. Lett.*, vol. 85, pp. 3966–3969, 2000.
- [41] <http://www.cmth.ph.ic.ac.uk/photonics/references.html>.
- [42] V. Veselago, “The electrodynamics of substances with simultaneously negative values of ϵ and μ ,” *Sov. Phys. Usp.*, vol. 10, pp. 509–514, 1968.

- [43] R. A. Shelby, D. R. Smith, and S. Schultz, “Experimental verification of a negative index of refraction,” *Science*, vol. 292, pp. 77–79, 2001.
- [44] D. R. Smith and N. Knoll, “Negative refractive index in left-handed materials,” *Phys. Rev. Lett.*, vol. 85, pp. 2933–2936, 2000.
- [45] C. Caloz, C.-C. Chang, and T. Itoh, “Full-wave verification of the fundamental properties of left-handed materials in waveguide configurations,” *J. Appl. Phys.*, vol. 90, no. 11, pp. 5483–5486, 2001.
- [46] R. W. Ziolkowski and E. Heyman, “Wave propagation in media having negative permittivity and permeability,” *Phys. Rev. E*, vol. 64, p. 056625, 2001.
- [47] R. Ziolkowski, “Design, fabrication and testing of double-negative metamaterials,” *IEEE Trans. Antennas Propag.*, vol. 51, pp. 1516–1529, 2003.
- [48] I. Lindell, S. Tretyakov, K. Nikoskinen, and S. Ilvonen, “BW media - media with negative parameters, capable of supporting backward waves,” *Microwave and Optical Technology Letters*, vol. 31, no. 10, pp. 129–133, 2001.
- [49] R. Ruppin, “Surface polaritons of a left-handed material slab,” *J. Phys.: Condens. Matter.*, vol. 13, pp. 1811–1819, 2001.
- [50] S. Foteinopolou, E. Economou, and C. Soukoulis, “Refraction in media with a negative refraction index,” *Phys. Rev. Lett.*, vol. 90, no. 10, p. 107402, 2003.
- [51] C. G. Parazzoli, R. B. Gregor, K. Li, B. E. C. Koltenbah, and M. Tanielian, “Experimental verification and simulation of negative index of refraction using snell’s law,” *Phys. Rev. Lett.*, vol. 90, p. 107401, 2003.
- [52] N. Engheta, “An idea for thin, subwavelength cavity resonators using metamaterials with negative permittivity and permeability,” *Ant. Wireless Propag. Lett.*, vol. 1, no. 1, pp. 10–13, 2002.
- [53] H. Lamb, “On group-velocity,” *Proc. London Math. Soc.*, vol. 1, pp. 473–479, 1904.
- [54] A. Schuster, *An Introduction to the Theory of Optics*. Edward Arnold, London, 1904.
- [55] H. Pocklington, “Growth of a wave-group when the group velocity is negative,” *Nature*, vol. 71, pp. 607–608, 1905.
- [56] G. Malyuzhinets, “A note on the radiation principle,” *Zh. Tekh. Fiz.*, vol. 21, pp. 940–942, 1951.

- [57] D. Sivukhin, “The energy of electromagnetic waves in dispersive media,” *Opt. Spektrosk.*, vol. 3, pp. 308–312, 1957.
- [58] L. Mandelshtam, “Group velocity in crystalline arrays,” *Zh. Eksp. Teor. Fiz.*, vol. 15, pp. 475–478, 1945.
- [59] L. Mandelshtam, *Complete works. Vol. 5.* Academy of Sciences, USSR, 1950.
- [60] *Special issue on Metamaterials of IEEE Trans. Antennas and Propagat.*, vol. 51, no. 10, 2003.
- [61] *Focus issue: Negative Refraction and Metamaterials, Optics Express*, vol. 11, no. 7, 2003.
- [62] *Metamaterials Exhibiting Left-Handed Properties and Negative Refraction, Progress In Electromagnetic Research, PIER*, vol. 51, 2005.
- [63] J. Pendry, “Manipulating the near field with metamaterials,” *Optics and Photonic News*, vol. 9, pp. 32–37, 2004.
- [64] D. Smith, J. Pendry, and M. Wiltshire, “Metamaterials and negative refraction index,” *Science*, vol. 305, pp. 788–792, 2004.
- [65] G. Marsh, “Topsy-turvy world of materials,” *Materials Today*, vol. 1, pp. 18–23, 2003.
- [66] S.A. Ramakrishna, “Physics of negative refractive index materials,” *Reports on Progress in Physics*, vol. 68, pp. 449–521, 2005.
- [67] <http://www.ee.duke.edu/~drsmith/>.
- [68] <http://ceta-p5.mit.edu/metamaterials/>.
- [69] <http://www.metamaterials-eu.org/>.
- [70] A. Houck, J. Brock, and I. Chuang, “Experimental verification of snell’s law in left-handed material,” *Phys. Rev. Lett.*, vol. 90, p. 137401, 2003.
- [71] T. Yen, W. Padilla, N. Fang, D. Vier, D. Smith, J. Pendry, D. Basov, and Z. Zhang, “Tetrahertz magnetic response from artificial materials,” *Science*, vol. 303, pp. 1494–1496, 2004.
- [72] S. Linden, C. Enkrich, M. Wegener, J. Zhou, T. Kochny, and C. Soukoulis, “Magnetic response of metamaterials at 100 tetrahertz,” *Science*, vol. 306, pp. 1351–1353, 2004.
- [73] T. Koschny, L. Zhang, and C. Soukoulis, “Isotropic three-dimensional left-handed metematerials,” *Phys. Rev. B*, vol. 71, p. 121103, 2005.

- [74] C. Simovski and S. He, “Frequency range and explicit expressions for negative permittivity and permeability of an isotropic medium formed by a lattice of perfectly conducting omega-particles,” *Phys. Lett. A*, vol. 311, pp. 254–263, 2003.
- [75] L. Ran, J. Huangfu, H. Chen, X. Zhang, K. Cheng, T. M. Grzegorzczak, and J. A. Kong, “Experimental study on several left-handed metamaterials,” *Progress In Electromagnetics Research, PIER*, vol. 51, pp. 249–279, 2005.
- [76] E. Verney, B. Sauviac, and C. Simovski, “Isotropic metamaterial electromagnetic lens,” *Phys. Lett. A*, vol. 331, pp. 244–247, 2004.
- [77] D. R. Smith and D. Schurig, “Electromagnetic wave propagation in media with indefinite permittivity and permeability tensors,” *Phys. Rev. Lett.*, vol. 90, no. 7, p. 077405, 2003.
- [78] D. R. Smith, P. Kolinko, and D. Schurig, “Negative refraction in indefinite media,” *J. Opt. Soc. Am. B*, vol. 21, no. 5, pp. 1032–1043, 2004.
- [79] D. R. Smith, D. Schurig, J. J. Mock, P. Kolinko, and P. Rye, “Partial focusing of radiation by a slab of indefinite media,” *Appl. Phys. Lett.*, vol. 84, no. 13, pp. 2244–2246, 2004.
- [80] *Mini-special issue on electromagnetic crystal structures, design, synthesis, and applications, IEEE Trans. Microwave Theory Techniques*, vol. 47, no. 11, 1999.
- [81] *Special Issue on Electromagnetic Applications of Photonic Band Gap Materials and Structures, Progress In Electromagnetic Research, PIER*, vol. 41, 2003.
- [82] K. Sakoda, *Optical Properties of Photonic Crystals*. Springer-Verlag, Berlin, 2005.
- [83] J. Joannopoulos, R. Mead, and J. Winn, *Photonic crystals: molding the flow of light*. Princeton University Press, NJ, 1995.
- [84] *Focus Issue: Photonic Bandgap Calculations, Optics Express*, vol. 8, no. 3, 2001.
- [85] *J. Opt. Soc. Am. B*, vol. 10, no. 2, pp. 280–413, 1993.
- [86] *Feature section on photonic crystal structures and applications of IEEE J. Quantum Electron.*, vol. 38, no. 7, 2002.
- [87] V. Agranovich and V. Ginzburg, *Spatial dispersion in crystal optics and the theory of excitons*. Wiley-Interscience, NY, 1966.
- [88] G. Agarwal, D. Pattanayak, and E. Wolf, “Electromagnetic fields in spatially dispersive media,” *Phys. Rev. B*, vol. 10, pp. 1447–1475, 1974.

- [89] J. L. Birman and J. J. Sein, “Optics of polaritons in bounded media,” *Phys. Rev. B*, vol. 6, pp. 2482–2490, 1972.
- [90] E. Yablonovitch, T. Gmitter, and K. Leung, “Photonic band structure: the face-centered-cubic case employing nonspherical atoms,” *Phys. Rev. Lett.*, vol. 67, no. 17, pp. 2295–2298, 1991.
- [91] E. Yablonovich, “Inhibited spontaneous emission in solid-state physics and electronics,” *Phys. Rev. Lett.*, vol. 58, no. 20, pp. 2059–2062, 1987.
- [92] S. John, “Strong localization of photons in certain disordered dielectric superlattices,” *Phys. Rev. Lett.*, vol. 58, no. 23, pp. 2486–2489, 1987.
- [93] <http://www.ee.ucla.edu/labs/photon/homepage.html>.
- [94] <http://www.physics.utoronto.ca/~john/>.
- [95] V. P. Bykov, “Spontaneous emission in a periodic structure,” *Sov. Phys. JETP*, vol. 35, pp. 269–273, 1972.
- [96] V. P. Bykov, “Spontaneous emission from a medium with a band spectrum,” *Sov. J. Quant. Electron*, vol. 4, pp. 861–871, 1975.
- [97] E. Yablonovitch and T. Gmitter, “Photonic band structure: the face-centered-cubic case,” *Phys. Rev. Lett.*, vol. 63, no. 18, pp. 1950–1953, 1989.
- [98] E. Yablonovitch and T. Gmitter, “Photonic band structure: the face-centered-cubic case,” *J. Opt. Soc. Am. A*, vol. 7, no. 9, pp. 1792–1800, 1990.
- [99] E. Yablonovitch, T. Gmitter, K. Leung, R.D.Meade, A. Rappe, K. Brommer, and J. Joannopoulos, “3-dimensional photonic band structure,” *Optical and Quantum Electronics*, vol. 24, no. 2, pp. 273–283, 1992.
- [100] E. Yablonovitch, “Photonic band-gap structures,” *J. Opt. Soc. Am. B*, vol. 10, no. 2, pp. 283–295, 1993.
- [101] J. Pendry, “Playing tricks with light,” *Science*, vol. 285, pp. 1687–1688, 1999.
- [102] <http://www.pbglink.com/>.
- [103] <http://phys.lsu.edu/~jdowling/pbgbib.html>.
- [104] J. Pendry, “Calculating photonic bandgap structure,” *J. Phys.: Condensed Matter*, vol. 8, no. 9, pp. 1085–1108, 1996.

- [105] D. Sievenpiper, L. Zhang, R. F. J. Broas, N. G. Alexopolous, and E. Yablonovitch, “High-impedance electromagnetic surfaces with a forbidden frequency band,” *IEEE Trans. Microwave Theory Techniques*, vol. 47, no. 11, pp. 2059–2074, 1999.
- [106] D. Sievenpiper, J. Schaffner, R. Loo, G. Tangonan, S. Ontiveros, and R. Harold, “A tunable impedance surface performing as a reconfigurable beam steering reflector,” *IEEE Trans. Antennas and Propagat.*, vol. 50, no. 3, pp. 384–390, 2002.
- [107] F.-R. Yang, K. P. Ma, Y. Qian, and T. Itoh, “A novel tem waveguide using uniplanar compact photonic band-gap (uc-pbg) structure,” *IEEE Trans. Microwave Theory Techniques*, vol. 47, no. 11, pp. 2092–2098, 1999.
- [108] S. Tretyakov and C. Simovski, “Wire antennas near artificial impedance surfaces,” *Microw. Optical Technology Lett.*, vol. 27, no. 1, pp. 46–50, 2000.
- [109] D. Sievenpiper, “High-impedance electromagnetic surfaces,” Ph.D. Dissertation, UCLA, 1999 (available at www.ee.ucla.edu/labs/photon/thesis/ThesisDan.pdf).
- [110] J. C. M. Garnett, “Colours in metal glasses and in metallic films,” *Phil. Trans. R. Soc. London*, vol. 203, pp. 385–420, 1904.
- [111] M. Born and E. Wolf, *Principles of optics*. University press, Cambridge, 1999.
- [112] S. Tretyakov, “Electrodynamics of bi-isotropic and bi-anisotropic media,” D.Sc. dissertation, St. Petersburg Polytechnical University, Russia, 1995.
- [113] S. Tretyakov, *Analytical modeling in applied electromagnetics*. Norwood, MA: Artech House, 2003.
- [114] L. Felsen and N. Marcuvitz, *Radiation and scattering of waves*. Prentice-Hall, Englewood Cliffs, NJ, 1972.
- [115] J. R. Wait, “Reflection at arbitrary incidence from a parallel wire grid,” *Appl. Sci. Res.*, vol. B IV, pp. 393–400, 1954.
- [116] J. R. Wait, “Reflection from a wire grid parallel to a conducting plane,” *Can. J. Phys.*, vol. 32, pp. 571–579, 1954.
- [117] V. Yatsenko, S. Tretyakov, S. Maslovski, and A. Sochava, “Higher order impedance boundary conditions for sparse wire grids,” *IEEE Trans. Antennas and Propagat.*, vol. 48, no. 5, pp. 720–727, 2000.
- [118] C. Poulton, S. Guenneau, and A. Movchan, “Noncommuting limits and effective properties for oblique propagation of electromagnetic waves through an array of aligned fibers,” *Phys. Rev. B*, vol. 69, p. 195112, 2004.

- [119] J. Sipe and J. V. Kranendonk, “Macroscopic electromagnetic theory of resonant dielectrics,” *Phys. Rev. A*, vol. 9, pp. 1806–1822, 1974.
- [120] A. Moroz, “Three-dimensional complete photonic-band-gap structures in the visible,” *Phys. Rev. Lett.*, vol. 83, no. 25, pp. 5274–5277, 1999.
- [121] S. Maslovski, S. Tratyakov, and P. Belov, “Wire media with negative effective permittivity: a quasi-static model,” *Microw. Optical Technology Lett.*, vol. 35, no. 1, pp. 47–51, 2002.
- [122] M. G. Silveirinha and C. A. Fernandes, “A hybrid method for the efficient calculation of the band structure of 3-d metallic crystals,” *IEEE Trans. Microw. Theory Techn.*, vol. 52, no. 3, pp. 889–902, 2004.
- [123] M. Silveirinha and C. Fernandes, “Homogenization of 3d- connected and non-connected wire metamaterials,” *IEEE Trans. Microw. Theory Techn.*, vol. 54, no. 4, pp. 1418–1430, 2005.
- [124] M. Silveirinha and C. Fernandes, “Homogenization of metamaterial surfaces and slabs: The crossed wire mesh canonical problem,” *IEEE Trans. Antennas Propagat.*, vol. 53, no. 1, pp. 59–69, 2005.
- [125] D. F. Sievenpiper, M. E. Sickmiller, and E. Yablonovitch, “3d wire mesh photonic crystals,” *Phys. Rev. Lett.*, vol. 76, pp. 2480–2483, 1996.
- [126] R. Silin and I. Chepurnykh, “On media with negative dispersion,” *Journal of Communications Technology and Electronics*, vol. 46, no. 10, pp. 1121–1125, 2001.
- [127] R. Silin, “Optical properties of artificial dielectrics,” *Izv. VUZ Radiofiz.*, vol. 15, pp. 809–820, 1972.
- [128] M. Notomi, “Theory of light propagation in strongly modulated photonic crystals: refractionlike behavior in the vicinity of the photonic band gap,” *Phys. Rev. B*, vol. 62, no. 16, pp. 10 696–10 705, 2000.
- [129] M. Notomi, “Negative refraction in photonic crystals,” *Optical and Quantum Electronics*, vol. 34, pp. 133–143, 2002.
- [130] R. Silin, *Unusual laws of refraction and reflection*. Moscow: Fazis, 1999.
- [131] R. Silin, *Periodical waveguides*. Moscow: Fazis, 2002.
- [132] P. Yeh, “Electromagnetic propagation in birefringent layered media,” *J. Opt. Soc. Am.*, vol. 69, no. 5, pp. 742–756, 1979.

- [133] S. Tretyakov, “Meta-materials with wideband negative permittivity and permeability,” *Microw. Optical Techn. Lett.*, vol. 31, no. 3, pp. 163–165, 2001.
- [134] S. Tretyakov, “Electromagnetic field energy density in artificial microwave materials with strong dispersion and loss,” *Phys. Letters A*, vol. 343, pp. 231–237, 2005.
- [135] C. Luo, S. G. Johnson, J. D. Joannopoulos, and J. B. Pendry, “All-angle negative refraction without negative effective index,” *Phys. Rev. B*, vol. 65, p. 201104, 2002.
- [136] Y. Zhang, B. Fluegel, and A. Mascarenhas, “Total negative refraction in real crystals for ballistic electrons and light,” *Phys. Rev. Lett.*, vol. 91, no. 15, p. 157404, 2003.
- [137] Z. Liu, Z. Lin, and S. Chui, “Negative refraction and omnidirectional total transmission at a planar interface associated with a uniaxial medium,” *Phys. Rev. B*, vol. 69, p. 115402, 2004.
- [138] R. Gajic, R. Meisels, F. Kuchar, and K. Hingerl, “Refraction and rightness in photonic crystals,” *Optics Express*, vol. 13, no. 21, pp. 8596–8605, 2005.
- [139] S. Forteinopoulou and C. Soukoulis, “Electromagnetic wave propagation in two-dimensional photonic crystals: A study of anomalous refractive effects,” *Phys. Rev. B*, vol. 72, p. 165112, 2005.
- [140] D. Smith, J. Pendry, and M. Wiltshire, “Metamaterials and negative refractive index,” *Science*, vol. 305, pp. 788–792, 2004.
- [141] S. Maslovski, S. Tretyakov, and P. Alitalo, “Near-field enhancement and imaging in double planar polariton-resonant structures,” *Journal of Applied Physics*, vol. 96, no. 3, pp. 1293–1300, 2004.
- [142] S. Maslovski and S. Tretyakov, “Phase conjugation and perfect lensing,” *Journal of Applied Physics*, vol. 94, no. 7, pp. 4241–4243, 2003.
- [143] S. Foteinopolou and C. Soukoulis, “Negative refraction and left-handed behaviour in two-dimensional photonic crystals,” *Phys. Rev. B*, vol. 67, p. 235107, 2003.
- [144] P. Parimi, W. Lu, P. Vodo, J. Sokoloff, J. S. Derov, and S. Sridhar, “Negative refraction and left-handed electromagnetism in microwave photonic crystals,” *Phys. Rev. Lett.*, vol. 92, no. 12, p. 127401, 2004.
- [145] A. Efros and A. Pokrovsky, “Dielectric photonic crystal as medium with negative electric permittivity and magnetic permeability,” *Solid State Commun.*, vol. 129, pp. 643–647, 2004.

- [146] C. Luo, S. G. Johnson, J. D. Joannopoulos, and J. B. Pendry, “Subwavelength imaging in photonic crystals,” *Phys. Rev. B*, vol. 68, p. 045115, 2003.
- [147] P. V. Parimi, W. T. Lu, P. Vodo, and S. Sridhar, “Imaging by flat lens using negative refraction,” *Nature*, vol. 426, p. 404, 2003.
- [148] X. Wang, Z. Ren, and K. Kempa, “Unrestricted superlensing in a triangular two-dimensional photonic crystals,” *Optics Express*, vol. 12, no. 13, pp. 2919–2924, 2004.
- [149] E. Cubukcu, A. K. E. Ozbay, S. Foteinopolou, and C. Soukoulis, “Subwavelength resolution in a two-dimensional photonic-crystal-based superlens,” *Phys. Rev. Lett.*, vol. 91, no. 20, p. 207401, 2003.
- [150] X. Zhang, “Absolute negative refraction and imaging of unpolarized electromagnetic waves by two-dimensional photonic crystals,” *Phys. Rev. B*, vol. 70, p. 205102, 2004.
- [151] C. Luo, S. G. Johnson, and J. D. Joannopoulos, “Negative refraction without negative index in metallic photonic crystals,” *Optics Express*, vol. 11, no. 7, pp. 746–754, 2003.
- [152] B. C. Gupta and Z. Ye, “Disorder effects on the imaging of a negative refractive lens made by array of dielectric cylinders,” *Journal of Applied Physics*, vol. 94, no. 4, pp. 2173–2176, 2003.
- [153] C. Luo, S. G. Johnson, and J. D. Joannopoulos, “All-angle negative refraction in three-dimensionally periodic photonic crystal,” *Appl. Phys. Lett.*, vol. 81, no. 13, pp. 2352–2354, 2002.
- [154] R. Moussa, S. Foteinopoulou, L. Zhang, G. Tuttle, K. Guven, E. Ozbay, and C. Soukoulis, “Negative refraction and superlens behavior in a two-dimensional photonic crystal,” *Phys. Rev. B*, vol. 71, p. 085106, 2005.
- [155] X. Wang and K. Kempa, “Effects of disorder on subwavelength lensing in two-dimensional photonic crystal slabs,” *Phys. Rev. B*, vol. 71, p. 085101, 2005.
- [156] X. Zhang, “Image resolution depending on slab thickness and object distance in a two-dimensional photonic-crystal-based superlens,” *Phys. Rev. B*, vol. 70, p. 195110, 2004.
- [157] A. Berrier, M. Mulot, M. Swillo, M. Qiu, L. Thylen, A. Talneau, and S. Anand, “Negative refraction at infrared wavelengths in a two-dimensional photonic crystal,” *Phys. Rev. Lett.*, vol. 93, no. 7, p. 073902, 2004.
- [158] A. Martinez, H. Miguez, A. Griol, and J. Marti, “Experimental and theoretical analysis of the self-focusing of light by a photonic crystal lens,” *Phys. Rev. B*, vol. 69, p. 165119, 2004.

- [159] K. Guven, K. Aydin, K. Alici, C. Soukoulis, and E. Ozbay, “Spectral negative refraction and focusing analysis of a two-dimensional left-handed photonic crystal lens,” *Phys. Rev. B*, vol. 70, p. 205125, 2004.
- [160] D. N. Chigrin, S. Enoch, C. M. S. Torres, and G. Tayeb, “Self-guiding in two-dimensional photonic crystals,” *Optics Express*, vol. 11, no. 10, pp. 1203–1211, 2003.
- [161] H.-T. Chien, H.-T. Tang, C.-H. Kuo, C.-C. Chen, and Z. Ye, “Directed diffraction without negative refraction,” *Phys. Rev. B*, vol. 70, p. 113101, 2004.
- [162] J. Witzens, M. Loncar, and A. Scherer, “Self-collimation in planar photonic crystals,” *IEEE Journal of Selected Topics in Quantum Electronics*, vol. 8, no. 6, pp. 1246–1257, 2002.
- [163] Z.-Y. Li and L.-L. Lin, “Evaluation of lensing in photonic crystal slabs exhibiting negative refraction,” *Phys. Rev. B*, vol. 68, p. 245110, 2003.
- [164] J. L. Garcia-Pomar and M. Nieto-Vesperinas, “Waveguiding, collimation and sub-wavelength concentration in photonic crystals,” *Optics Express*, vol. 13, no. 20, pp. 7997–8007, 2005.
- [165] C.-H. Kuo and Z. Ye, “Optical transmission of photonic crystal structures formed by dielectric cylinders: Evidence for non-negative refraction,” *Phys. Rev. E*, vol. 70, p. 056608, 2004.
- [166] R. W. Ziolkowski, “Propagation in and scattering from a matched metamaterial having a zero index of refraction,” *Phys. Rev. E*, vol. 70, p. 046608, 2004.
- [167] L. Chen, S. He, and L. Shen, “Finite-size effects of a left-handed material slab on the image quality,” *Phys. Rev. Lett.*, vol. 92, no. 10, p. 107404, 2004.
- [168] C. Simovski and S. He, “Antennas based on modified metallic photonic bandgap structures consisting of capacitively loaded wires,” *Microw. Optical Techn. Lett.*, vol. 31, no. 5, pp. 214–221, 2001.
- [169] M. Wiltshire, J.B.Pendry, I. Young, D. Larkman, D. Gilderdale, and J. Hajnal, “Microstructured magnetic materials for radio frequency operation in magnetic resonance imaging (mri),” *Science*, vol. 291, pp. 849–851, 2001.
- [170] M. Wiltshire, J. Hajnal, J.B.Pendry, and D. Edwards, “Metamaterial endoscope for magnetic field transfer: near field imaging with magnetic wires,” *Optics Express*, vol. 11, pp. 709–715, 2003.
- [171] S. A. Ramakrishna, J. B. Pendry, M. C. K. Wiltshire, and W. J. Stewart, “Imaging the near field,” *Journal of Modern Optics*, vol. 50, pp. 1419–1430, 2003.

- [172] S. A. Ramakrishna and J. B. Pendry, “Removal of absorption and increase in resolution in a near-field lens via optical gain,” *Phys. Rev. B*, vol. 67, p. 201101, 2003.
- [173] J. T. Shen, P. B. Catrysse, and S. Fan, “Mechanism for designing metallic metamaterials with a high index of refraction,” *Phys. Rev. Lett.*, vol. 94, p. 197401, 2005.
- [174] E. Shamonina, V. Kalinin, K. Ringhofer, and L. Solymar, “Imaging, compression and poynting vector streamlines for negative permittivity materials,” *Electron. Lett.*, vol. 37, pp. 1243–1244, 2001.
- [175] F. J. G. de Abajo, G. Gomez-Santos, L. A. Blanco, A. G. Borisov, and S. V. Shabanov, “Tunneling mechanism of light transmission through metallic films,” *Phys. Rev. Lett.*, vol. 95, p. 067403, 2005.
- [176] W. Cai, D. A. Genov, and V. M. Shalaev, “Superlens based on metal-dielectric composite,” *Phys. Rev. B*, vol. 72, p. 193101, 2005.

- S 270 Chicherin, D., Tretyakov, S.
Third annual SMARAD centre of excellence research seminar, April 2005
- S 271 Räisänen, A.V., Jääskeläinen, A.
SMARAD Smart and Novel Radios Research Unit Activity Report 2002-2004,
June 2005
- S 272 Kivekäs (née Lehmus), O.
Design of high-efficiency antennas for mobile communications devices,
August 2005
- S 273 Laitinen, T.
Advanced spherical antenna measurements, December 2005
- S 274 Salonen, I., Icheln, C., Vainikainen, P.
Beamforming with wide null sectors for realistic arrays using directional
weighting, December 2005
- S 275 Räisänen, A.V., Lindberg, S.
TKK Radio Laboratory research and education 2005, March 2006
- S 276 Salonen, I.
Evaluation and compensation of mutual coupling and other non-idealities in
small antenna arrays, May 2006
- S 277 Suvikunnas, P., Salo, J., Vuokko, L. Kivinen, J., Sulonen, K., Vainikainen, P.
Comparison of MIMO antenna configurations: Methods and experimental
results, June 2006
- S 278 Salo, J.
Statistical analysis of the wireless propagation channel and its mutual
information, July 2006
- S 279 Suvikunnas, P.
Methods and criteria for performance analysis of multiantenna systems in
mobile communications, August 2006
- S 280 Tretyakov, S., Alitalo, P.
International student seminar on microwave applications of novel physical
phenomena, August 2006
- S 281 Häkli, J.
Shaped reflector antenna design and antenna measurements at sub-mm
wavelengths, September 2006
- S 282 Lönnqvist, A.
Applications of hologram-based compact range: Antenna radiation pattern,
radar cross section, and absorber reflectivity measurement, September 2006
- S 283 Tretyakov, S., Osipov, A.
Applied theory of electromagnetic scattering and diffraction, September 2006